Molecular mechanisms of regulation of fast-inactivating voltage-dependent transient outward K^+ current in mouse heart by cell volume changes

Guan-Lei Wang, Ge-Xin Wang, Shintaro Yamamoto, Linda Ye, Heather Baxter, Joseph R. Hume and Dayue Duan

Center of Biomedical Research Excellence, Department of Pharmacology, University of Nevada School of Medicine, Reno, NV 89557-0270, USA

The $K_v4.2/4.3$ channels are the primary subunits that contribute to the fast-inactivating, voltage-dependent transient outward K^+ current ($I_{to,fast}$) in the heart. $I_{to,fast}$ is the critical determinant of the early repolarization of the cardiac action potential and plays an important role in the adaptive remodelling of cardiac myocytes, which usually causes cell volume changes, during myocardial ischaemia, hypertrophy and heart failure. It is not known, however, whether $I_{to,fast}$ is regulated by cell volume changes. In this study we investigated the molecular mechanism for cell volume regulation of $I_{to,fast}$ in native mouse left ventricular myocytes. Hyposmotic cell swelling caused a marked increase in densities of the peak $I_{to,fast}$ and a significant shortening in phase 1 repolarization of the action potential duration. The voltage-dependent gating properties of $I_{to,fast}$ were, however, not altered by changes in cell volume. In the presence of either protein kinase C (PKC) activator (12,13-dibutyrate) or phosphatase inhibitors (calyculin A and okadaic acid), hyposmotic cell swelling failed to further up-regulate $I_{to,fast}$. When expressed in NIH/3T3 cells, both $K_v4.2$ and $K_v4.3$ channels were also strongly regulated by cell volume in the same voltage-independent but PKC- and phosphatase-dependent manner as seen in $I_{to,fast}$ in the native cardiac myocytes. We conclude that $K_v4.2/4.3$ channels in the heart are regulated by cell volume through a phosphorylation/dephosphorylation pathway mediated by PKC and serine/threonine phosphatase(s). These findings suggest a novel role of $K_v4.2/4.3$ channels in the adaptive electrical and structural remodelling of cardiac myocytes in response to myocardial hypertrophy, ischaemia and reperfusion.

(Resubmitted 24 May 2005; accepted after revision 28 July 2005; first published online 4 August 2005)
Corresponding author D. Duan: Center of Biomedical Research Excellence, Department of Pharmacology, University of Nevada School of Medicine, Manville Medical Building Room no. 9/MS 318, Reno, NV 89557-0270, USA. Email: dduan@med.unr.edu

The Ca^{2+}-independent, fast-inactivating, transient outward K^+ current ($I_{to,1}$ or $I_{to,fast}$) is the critical determinant of the early (phase 1) repolarization of the action potential duration (APD) and excitation–contraction (E–C) coupling of the heart in many mammalian species, including human (Nerbonne & Guo, 2002; Sah *et al.* 2003). The primary subunits that contribute to $I_{to,fast}$ are the $K_v4.2$ or $K_v4.3$ channels, or a combination of the two (Dixon *et al.* 1996; Johns *et al.* 1997; Hoppe *et al.* 2000). Recently, it has been suggested that decreased expression of $K_v4.2/4.3$ may be responsible for the decreased $I_{to,1}$ density and prolonged APD in many animal models of heart diseases and in human heart failure as well (Takimoto *et al.* 1997; Kaab *et al.* 1998; Huang *et al.* 2000; Kassiri *et al.* 2002). The mechanism underlying the link between the ionic remodelling (reduction in $I_{to,1}$ density and $K_v4.2/4.3$ expression) and structural remodelling (myocardial hypertrophy and dilated heart failure) remains to be elucidated.

In response to myocardial hypertrophy and heart failure, adaptive remodelling of the cardiac myocytes is closely associated with perturbations of both cell volume and ion channel function (Frey *et al.* 2004; Duan *et al.* 2005). Other pathological stress such as myocardial hypoxia, ischaemia and reperfusion also causes alterations in cell volume and ion channel activities due to changes in extracellular osmolarity (Steenbergen *et al.* 1985; Wright & Rees, 1998; Befroy *et al.* 1999). Excessive cell volume changes in the heart may cause profound alteration of structural integrity and constancy of the intracellular milieu, which in turn will affect many cellular functions, including: cardiac electrical activity and contractility due to changes in membrane ion permeability (Vandenberg *et al.* 1996; Wright & Rees, 1998; Befroy *et al.* 1999; Kocic

 DOI: 10.1113/jphysiol.2005.091264

et al. 2001; Baumgarten & Clemo, 2003; Frey *et al.* 2004); intracellular metabolism (Wright & Rees, 1998; Kocic *et al.* 2001; Baumgarten & Clemo, 2003); and multiple intracellular signal cascades including protein kinase C (PKC) and protein phosphatases (Wright & Rees, 1998; Duan *et al.* 1999*a*; Lang *et al.* 2000; Baumgarten & Clemo, 2003; Dorn & Force, 2005). In fact, it has been consistently shown that hyposmotic cell swelling causes significant shortening in APD of both atrial and ventricular myocytes (Vandenberg *et al.* 1997; Kocic *et al.* 2001; Duan *et al.* 2005). Although activation of the volume-regulated Cl^- current ($I_{Cl,vol}$) (Duan *et al.* 1997*a*,*b*, 1999*a*; Vandenberg *et al.* 1997), the slow delayed rectifier ($I_{K,s}$) (Rees *et al.* 1995), the ATP-sensitive K^+ current ($I_{K,ATP}$) (Priebe & Beuckelmann, 1998), and the Cl^- inward rectifier ($I_{Cl,ir}$) (Duan *et al.* 2000), has been reported to contribute to cell swelling-induced APD shortening (Hiraoka *et al.* 1998; Kocic *et al.* 2001), the mechanism for the shortening in early phase 1 repolarization of APD remains unclear. It is not known whether $I_{to,fast}$ is regulated by cell volume changes, and whether the shortening in phase 1 of cardiac APD is due to cell swelling-induced up-regulation of $I_{to,fast}$ (Vandenberg *et al.* 1996; Hiraoka *et al.* 1998; Wright & Rees, 1998; Kocic *et al.* 2001).

In mouse cardiac myocytes isolated from the apex of left ventricle, previous studies have identified at least four distinct voltage-dependent K^+ currents, namely the fast transient outward K^+ current ($I_{to,fast}$), the ultra-rapidly activating, slowly inactivating delayed rectifier K^+ current ($I_{K,slow1}$), the TEA-sensitive slowly activating delayed rectifier K^+ current ($I_{K,slow2}$) and the non-inactivating steady-state current (I_{ss}). In addition to their distinct molecular identities these K^+ currents can be effectively separated for the purpose of functional characterization in cardiac myocytes by using a combination of biophysical and pharmacological approaches (Brouillette *et al.* 2004). In this study, we adapted these valid approaches to isolate $I_{to,fast}$ from other K^+ currents (e.g. $I_{K,slow1}$, $I_{K,slow2}$ and I_{ss}) in cardiac myocytes of mouse left ventricle apex and investigated cell volume regulation of $I_{to,fast}$. We found that $I_{to,fast}$ and its key molecular components, both $K_v4.2$ and $K_v4.3$ channels, are strongly regulated by cell volume through a phosphorylation and dephosphorylation mechanism mediated by PKC and serine/threonine phosphatase(s). These results suggest a novel role of $K_v4.2/4.3$ channels in electrical remodelling caused by cell volume changes such as cell swelling and hypertrophy, and thus provide an alternative mechanism for their function in heart diseases.

Methods

The investigation conforms to the *Guide for the Care and Use of Laboratory Animals* published by the US National Institutes of Health (NIH Publication No. 85-23, revised 1996) and was in accordance with the institutional guidelines for animal care and use approved by the University of Nevada, Reno Institutional Animal Care and Use Committee.

Isolation of single cardiac myocytes

Single cardiac myocytes were isolated from left ventricular apex of adult mice (C57/BL, male, 25–30 g) using a well-established method as previously described (Duan *et al.* 1993, 1999*b*, 2000). Briefly, the animals were anaesthetized by injection of sodium phenobarbitone (50 mg kg^{-1}, I.P.) until a surgical level of anaesthesia was confirmed by loss of withdrawal reflex to toe pinch. A thoracotomy was then performed; the heart was quickly removed and perfused in a Langendorff mode, first with normal Tyrode solution and then with Ca^{2+}-free Tyrode solution until heart beating completely ceased. The hearts were then perfused with the same Ca^{2+}-free Tyrode solution but containing 0.04% collagenase type 2 (Worthington, Biochemical, Lakewood, NJ, USA Co.) for 10–15 min. The left ventricular apex was removed and isolated myocytes were harvested. Only Ca^{2+}-tolerant quiescent myocytes with a typical rod-shaped form and clear cross-striations were used for experiments. Cell dimensions (diameter or width and length) were monitored with two calibrated graticules (one for width and the other for length) in the microscope and cell volume was estimated with assumed right cylindrical geometry according to the following equation: $V = \pi L(D/2)^2$, where V, L and D are cell volume, length and diameter, respectively (Duan *et al.* 1997*a*).

Expression of $K_v4.2$ and $K_v4.3$ in NIH/3T3 mammalian cells

The cDNA of rat $K_v4.3$ long form ($rK_v4.3$ l, Genebank accession number AB003587) and rat $K_v4.2$ (Genebank accession number M59980) (generous gifts from Dr Susumu Ohya, Department of Molecular & Cellular Pharmacology, Nagoya City University, Japan) were transfected into NIH/3T3 cells by Lipofectamine 2000 (Invitrogen, Carlsbad, CA, USA). NIH/3T3 cells (American Type Culture Collection, Rockville, MD, USA) were maintained in Dulbecco's modified Eagle's medium supplemented with 5% fetal calf serum (Invitrogen). The day before transfection, cells were trypsinized and plated into 24-well plates at 1.5×10^5 cells per well so that they were 90–95% confluent on the day of transfection. Stable transfectants were selected by 1000 μg ml^{-1} G418 (Invitrogen). Individual G418-resistant subclones were isolated, expanded and maintained. Cells were grown on sterile glass coverslips for 1 day and then used for patch-clamping experiments.

Solutions

For current-clamp and voltage-clamp experiments shown in Fig. 1, the hyposmotic bath solution contained (mM): sodium aspartate, 110; potassium aspartate, 5.4; $MgCl_2$, 0.8; $CaCl_2$, 1; NaCl, 10; glucose, 10; Hepes, 10; pH 7.2, 235 mosmol kg^{-1}. The isosmotic bath solutions were the same except that the osmolarity was adjusted to 305 mosmol kg^{-1} by adding mannitol. The pipette solution contained (mM): KCl, 20; potassium aspartate, 120; Mg-ATP, 5; EGTA, 10; Hepes, 10; pH 7.2, 290 mosmol kg^{-1}. A high concentration of ATP (5 mM) in the pipette solution was used to prevent the activation of K_{ATP} and its contribution to APD. For the rest of the voltage-clamp experiments, bath and pipette solutions were chosen to facilitate I_{to} recording and to eliminate contaminations from other currents. The standard hyposmotic bath solution contained (mM): *N*-methyl-D-glucamine (NMDG), 85; L-aspartaric acid, 95; $CdCl_2$, 0.3; $MgCl_2$, 0.8; $BaCl_2$, 2; $CaCl_2$, 1; KCl, 5.4; TEA-Cl, 10; glucose, 10; Hepes, 10; pH 7.2, 235 mosmol kg^{-1}. The isosmotic and hyperosmotic bath solutions were the same as the hyposmotic bath solution except that the osmolarity was adjusted by adding mannitol to 305 and 350 mosmol kg^{-1}, respectively. The standard pipette solution contained (mM): KCl, 20; potassium aspartate, 120; Mg-ATP, 5; EGTA, 10; Hepes, 10; pH 7.2, 290 mosmol kg^{-1}. EGTA (10 mM) was included in the pipette solution and Cd^{2+} (0.3 mM), Ba^{2+} (2 mM) and TEA-Cl (10 mM) were present continuously in the bath solution to block L-type Ca^{2+} current ($I_{Ca,L}$, Ca^{2+})-dependent outward K^+ and Cl^- currents, K^+ inward rectifiers (I_{K1}), and delayed rectifiers ($I_{K,s}$, $I_{K,r}$ and $I_{K,slow2}$), respectively (Duan *et al.* 1993, 1999*b*, 2000; Zhou *et al.* 2003). Extracellular Na^+ was eliminated to preclude the contamination by Na^+ current (I_{Na}). Low Cl^- concentrations on both extracellular ($[Cl^-]_o = 21.6$ mM) and intracellular ($[Cl^-]_i = 20$ mM) sides were used to minimize contamination from the swelling-activated Cl^- currents ($I_{Cl,swell}$) and $I_{Cl,ir}$ (Duan *et al.* 1997*a*,*b*, 2000) and the Ca^{2+}-activated Cl^- current ($I_{Cl,Ca}$ or $I_{to,2}$) in mouse ventricular myocytes (Xu *et al.* 2002). The osmolarity of all solutions was measured just before each experiment by the Advanced Microosmometer 3300 (Advanced Instruments, Inc., Norwood, MA, USA). Isosmotic (1*T*; where *T* is relative osmolarity) solution was set as 305 mosmol kg^{-1}. Therefore, the hyposmotic solutions were 0.77*T* (235/305 mosmol kg^{-1}) and the hyperosmotic solutions were 1.15*T* (350/305 mosmol kg^{-1}). All chemicals were purchased from Sigma.

Electrophysiological measurements and data analysis

The tight-seal, whole-cell current-clamp and voltage-clamp techniques as previously described (Hamill *et al.* 1991; Duan *et al.* 1997*a*,*b*, 1999*b*, 2000) were used to record action potentials and whole-cell currents, respectively, from single mouse ventricular myocytes. Voltage-clamp and current-clamp recordings were obtained using an Axopatch 200 A patch-clamp amplifier (Axon Instruments, Inc., Union City, CA, USA). Data acquisition and command potentials were controlled by pCLAMP 8.0 software (Axon Instruments). Currents were recorded from a holding potential of −60 mV to a series of test potentials from −50 to +80 mV for 1 s in +10 mV increments at an interval of 10 s. Whole-cell currents were filtered at 1 kHz and sampled at 5 kHz. Action potentials were recorded simultaneously from the same myocytes using a brief stimulus (2-ms depolarizing current) at a frequency of 5 Hz under the same conditions for the recording of outward K^+ currents. Recording pipettes were prepared from borosilicate glass electrodes (1.5 mm

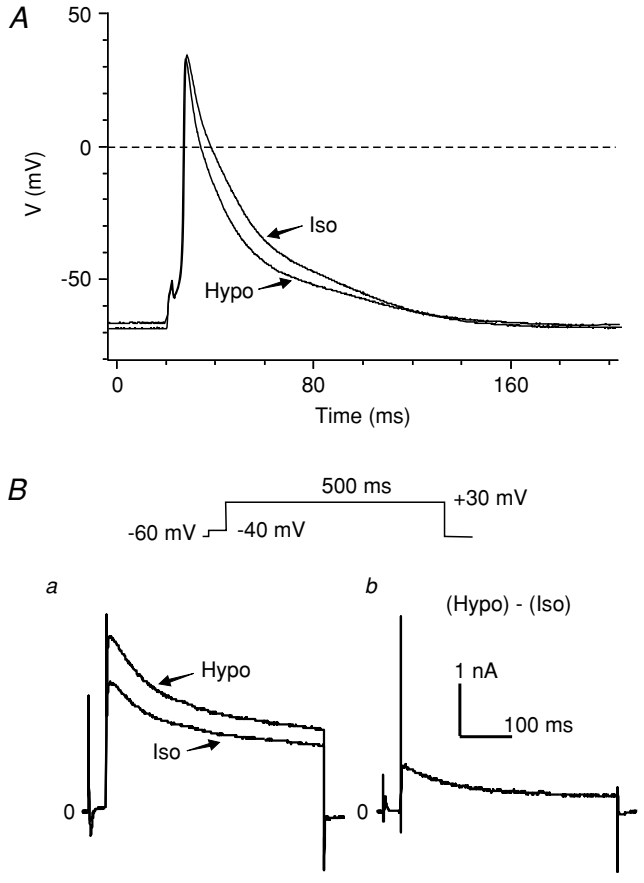

Figure 1. Osmotic regulation of APD and I_{to} in mouse left ventricular apex myocytes
A, superimposed representative action potential recordings under isosmotic (Iso, 305 mosmol kg^{-1}) and hyposmotic (Hypo, 235 mosmol kg^{-1}) conditions. *B*, original traces of whole-cell currents measured in the same cell as in panel *A*. *a*, superimposed representative whole-cell current traces recorded with the voltage protocols shown above, under isosmotic (Iso) and hyposmotic (Hypo) conditions. *b*, hyposmotic stress-sensitive current obtained by subtracting the current recorded under isosmotic (Iso) conditions from that under hyposmotic (Hypo) conditions.

Table 1. Effects of hyposmotic cell swelling on action potential in mouse ventricular myocytes

	Resting potential (mV)	APD (ms)	APD_{25} (ms)	APD_{75} (ms)	APD_{90} (ms)
Isosmotic	-69.5 ± 1.6	95.1 ± 9.8	2.7 ± 0.5	18.0 ± 4.4	45.2 ± 7.9
Hyposmotic	-68.5 ± 1.2	58.4 ± 8.8**	1.8 ± 0.4*	13.7 ± 5.1*	25.3 ± 7.0**

* $P < 0.05$, * * $P < 0.01$ *versus* isosmotic ($n = 5$).

o.d.) with tip resistance of 1–3 MΩ when filled with pipette solutions. The cell capacitance was calculated by integrating the area under an uncompensated capacitive transient elicited by a 5-mV hyperpolarizing pulse from a holding potential of 0 mV. The whole-cell membrane capacitance of mouse left ventricular myocytes was 116 ± 14 pF ($n = 60$). To separate individual outward K^+ current components, currents were elicited by a +30-mV depolarizing step from a holding potential of −80 mV. The amplitude of test current components was measured as the difference between the peak current and the current level at the end of the voltage pulse. A conventional two-pulse protocol was used to analyse the effects of osmotic stress on the voltage dependence of the inactivation. For $I_{to,fast}$, cells were first clamped to different potentials ranging from −100 to 0 mV for 100 ms, and then followed by a 1-s test pulse to +30 mV. The amplitude of test current evoked from each prepulse potential was normalized to the maximal current amplitude (I_{max}) evoked from −100 mV (at which inactivation was completely removed), and plotted as a function of the inactivating prepulse potential. The inactivation curves obtained from the double-pulse protocol were fitted to the following Boltzmann equation: $y_\infty = 1/\{1 + \exp[(V_{pp} - V_{1/2})/k]\}$, where V_{pp} is the potential of the prepulse, $V_{1/2}$ is the membrane potential at 50% inactivation and k is the slope factor. The time course of recovery from inactivation was determined by a double-pulse stimulus protocol. The first depolarization pulse (P1) was applied from a holding potential of −80 mV to +30 mV for 500 ms (to completely inactivate the currents) followed by a second depolarization pulse (P2) to +30 mV for 500 ms with variable interpulse intervals at the holding potential. The test-current amplitudes evoked by P2 at +30 mV after each recovery period were normalized to the current amplitudes evoked by P1 in the same cell, and plotted against recovery time. Exponential functions were fitted to the data describing the recovery from inactivation. Details are given in Results. All experiments were conducted at room temperature (22–24 °C). To account for differences in cell size, whole-cell currents were normalized to cell capacitance, and the average data were reported as current densities (pA pF^{-1}). Group data are presented as means ± S.E.M. Student's t-test was used to determine statistical significance. A two-tailed probability (P) of ±5% was considered significant.

Results

Effects of osmotic stress on APD and transient outward K^+ currents in native mouse ventricular myocytes

To examine the cell swelling-induced APD changes in mouse ventricular myocytes and the corresponding changes in whole-cell currents, action potentials and whole-cell currents were recorded from the same cell using alternations of voltage-clamp and current-clamp modes under the same conditions. Representative superimposed action potential traces recorded from a ventricular myocyte exposed to isosmotic (Iso) and hyposmotic (Hypo) solutions for 10 min, respectively, are shown in Fig. 1*A*. Consistent with previous observations in cardiac myocytes of mouse and several other species (Hamill *et al.* 1991; Duan *et al.* 1995, 1997*a*,*b*, 1999*a*; Vandenberg *et al.* 1997; Kocic *et al.* 2001), exposure of mouse left ventricular myocytes to hyposmotic perfusates caused cell swelling (∼150% increase in cell size) (Duan *et al.* 1995, 2000), which was accompanied by a significant shortening in APD in all (five out of five) tested cells. Table 1 summarizes the changes in the action potential parameters under isosmotic and hyposmotic conditions. Hyposmotic cell swelling caused a significant shortening in APD, especially in the early repolarization phases as measured at 5% (APD_5) and 10% (APD_{10}) repolarization. APD_5 shortened $58 \pm 5\%$ and APD_{10} shortened $38 \pm 3\%$, respectively ($n = 5$, $P < 0.001$ *versus* isosmotic conditions). These changes were accompanied by a significant increase in the outward currents (Fig. 1*Ba*) under the same hyposmotic conditions. It has been previously reported that activation of several volume-sensitive currents, such as $I_{Cl,swell}$ (Duan *et al.* 1997*a*,*b*, 2000; Vandenberg *et al.* 1997), $I_{K,s}$ (Rees *et al.* 1995), $I_{K,ATP}$ (Priebe & Beuckelmann, 1998) and $I_{Cl,ir}$ (Duan *et al.* 2000), may be responsible for the swelling-induced shortening in APD but the mechanism for the shortening in early repolarization (APD_5 and APD_{10}) remains unclear. As shown in Fig. 1*Bb*, cell swelling-induced currents include a transient outward current, suggesting that cell swelling-induced increase in transient outward K^+ currents may contribute to the shortening in early repolarization.

In our experimental conditions, hyposmotic cell swelling failed to cause significant changes in resting membrane potential (RMP) (Table 1) and I_{K1} (data not

shown) in mouse ventricular myocytes. The measured mean RMP of the single adult mouse ventricular myocytes was -69.5 ± 1.6 mV ($n = 5$, Table 1), which is more positive than the predicted normal RMP (> -80 mV) of ventricular myocytes but is in very good agreement with the value of -64 to -68 mV measured also from adult mouse ventricular myocytes under similar experimental conditions by Nerbonne and colleagues (Barry *et al.* 1998; Xu *et al.* 1999*a*,*c*). The depolarized RMP recorded from a single ventricular myocyte may be due to a number of reasons, such as: the compositions of the bath and pipette solutions, the experimental temperature, the status of the isolated single adult mouse ventricular myocytes, etc. Therefore caution should be used when interpreting the action potential results recorded from a single cell. In our study of the effects of hyposmotic challenge on the action potentials, therefore, we designed a parallel control group to monitor the changes in action potentials when the cells were exposed to only isosmotic bath solutions for the same time course (at least 30 min). No significant changes in APD and outward current were found in the control group ($n = 4$, data not shown) while hyposmotic cell swelling caused a significant shortening in APD, especially the early phase of APD (Table 1). These observations are consistent with previous reports from many other laboratories (Vandenberg *et al.* 1997; Kocic *et al.* 2001; Duan *et al.* 2005).

The results shown in Fig. 1*Bb* are very intriguing because there is currently no information available in the literature about the cell volume regulation of transient outward currents in the heart or any other tissues. Given the well-documented crucial role of the transient outward K^+ currents in the early repolarization and E–C coupling (ECC) in human and numerous other animal models (Barry *et al.* 1998; Kaab *et al.* 1998; Wang *et al.* 1999; Yue *et al.* 1999; Huang *et al.* 2000), it is very important to determine whether or not these K^+ currents in cardiac myocytes are regulated by osmotic stress-induced cell volume changes. We therefore used experimental approaches that are well-established in our laboratory (Duan *et al.* 1993, 1995, 1997*a*,*b*, 1999*a*, 2000) to study the osmotic regulation of the transient outward currents. Figure 2*A* shows the time course of osmotic stress on the changes in cell volume and the transient outward peak current recorded in a single cell at $+40$ mV from a holding potential of -60 mV under isosmotic, hyposmotic and hyperosmotic conditions. Exposure to hyposmotic solutions caused a time-dependent cell swelling and increase in the peak current. As shown in Fig. 2*A*, cell volume started to increase <1 min after hyposmotic perfusion and reached steady state in 10 min. Peak current started to increase after 3 min perfusion with hyposmotic solutions and reached steady state after 15 min hyposmotic perfusion. In seven cells, hyposmotic challenge increased the mean cell volume from $12\,870 \pm 1488$ to $19\,217 \pm 2903\ \mu m^3$ ($143 \pm 7\%$ increase, $P < 0.01$, $n = 7$) and the peak current density from 24.7 ± 0.3 to 41.2 ± 0.4 pA pF^{-1} ($162 \pm 7\%$ increase, $P < 0.001$, $n = 7$). Hyperosmotic solution caused a time-dependent cell shrinkage ($9824 \pm 2903\ \mu m^3$, $n = 7$) and a decrease in the peak current density (20.4 ± 0.2 pA pF^{-1}, $n = 7$) after 20-min hyperosmotic perfusion. In all of these cells, there was usually a $\sim$2-min lag between changes in the peak current and the cell volume. The slower onset of the changes in I_{peak} strongly supports the notion that the regulation of I_{peak} by osmotic challenges is a result of cell volume changes, which may be working by affecting intracellular and/or cell membrane-bounded (for example, stretch of cytoskeleton) signalling transduction pathways.

Figure 2*B* shows a representative family of outward currents recorded in a myocyte under isosmotic (*a*), hyposmotic (*b*) and hyperosmotic (*c*) conditions. These osmotic stress-regulated outward currents are the Ca^{2+}-independent voltage-gated transient outward K^+ currents because: (1) contamination from other ionic channels such as $I_{K,r}$, $I_{K,s}$, $I_{K,slow2}$, I_{K1}, $I_{Ca,L}$, $I_{Cl,Ca}$, I_{Na} and $I_{Cl,swell}$ were eliminated or minimized by TEA, Ba^{2+}, Cd^{2+}, no Na^+, high intracellular EGTA (10 mM) and low concentrations of Cl^- (see Methods); and (2) the transient outward currents under hyposmotic conditions were significantly blocked by 4-aminopyridine (4-AP; 5 mM, data not shown). Chiamvimonvant and colleagues have discovered a Ca^{2+}-activated Cl^- channel in mouse heart (Xu *et al.* 2002). The Ca^{2+}-activated Cl^- current ($I_{Cl,Ca}$) is also called $I_{to,2}$ because its transient activation and inactivation properties are very similar to $I_{to,fast}$. Therefore, it is possible that activation of $I_{Cl,Ca}$ may also contribute to the shortening in early repolarization of cardiac APD observed in the ventricular myocytes. There is currently no information about the volume regulation of cardiac Ca^{2+}-activated Cl^- channels available in any species (Hume *et al.* 2000; Duan *et al.* 2005). In the present study, however, the possible contribution of $I_{Cl,Ca}$ to the observed cell volume regulation of I_{to} was eliminated by using a very high intracellular EGTA (10 mM) to buffer intracellular Ca^{2+} and very low concentrations of Cl^- in both pipette and bath solutions ($\sim$20 mM) to minimize Cl^- currents.

Figure 2*C* shows the mean current–voltage (*I–V*) relationship of osmotic-regulated peak (I_{peak}) and steady-state (I_{ss}) components of the outward K^+ current. The density of I_{peak} was measured as the difference between the peak current and the current level at the end of the voltage steps then normalized with the cell capacitance. The mean current density of I_{peak} was increased significantly by hyposmotic-induced cell swelling over the range of -30 to $+80$ mV, and the subsequent hyperosmotic cell shrinkage decreased the mean current density of I_{peak} significantly over the range of 0 to $+80$ mV.

For example, the current density of I_{peak} at +40 mV was 26.6 ± 1.3, 36.7 ± 1.6 and 21 ± 2.1 pA pF^{-1} ($n = 12$, $P < 0.01$), under isosmotic, hyposmotic and hyperosmotic conditions, respectively. The non-inactivating steady-state current that remains at the end of 4.5-s voltage steps is referred to as I_{ss} (Xu *et al.* 1999*b*). In contrast to I_{peak}, and as shown in Fig. 2*D*, I_{ss} was not affected by changes in osmotic conditions. For example, at +40 mV, the current

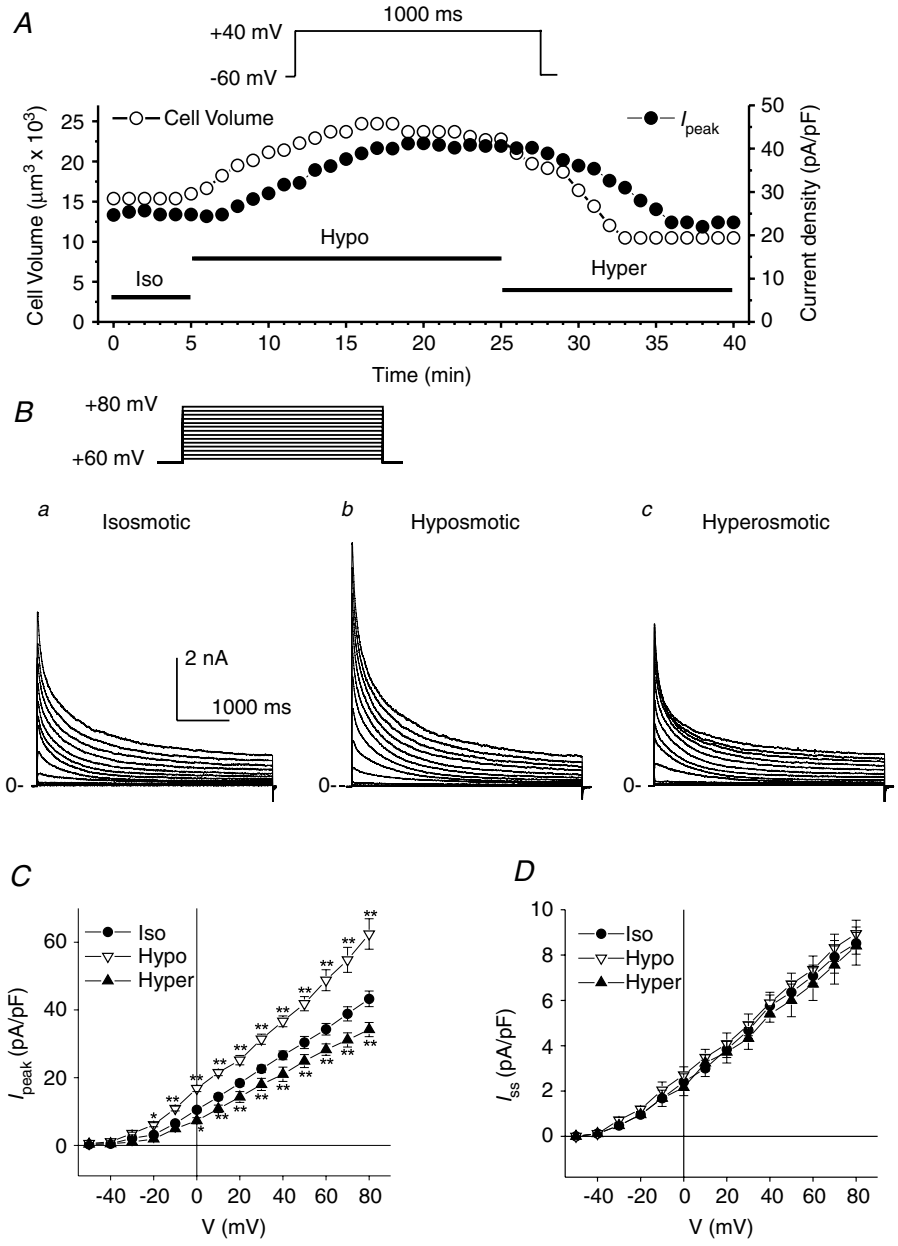

Figure 2. Effects of osmotic stress on cell volume and transient outward K^+ currents in mouse ventricular apex myocytes

A, representative time course of changes in cell volume (○, *y*-axis on the left) and peak transient outward K^+ current density (●, *y*-axis on the right) in a single mouse ventricular myocyte under different osmotic conditions. Cell volume and the whole-cell outward currents elicited by a 1-s depolarizing voltage pulse to +40 mV from a holding potential of −60 mV were continuously monitored every 1 min when the cell was exposed to isosmotic (Iso), hyposmotic (Hypo) and hyperosmotic (Hyper) solutions, respectively. Similar results were observed in seven cells. *B*, families of whole-cell outward currents elicited by a series of 4.5-s depolarizing voltage steps from a holding potential of −60 mV to potentials between −50 and +80 mV in 10-mV increments (inset on top) under isosmotic (*a*), hyposmotic (*b*) and hyperosmotic (c) conditions. *C* and *D*, mean *I–V* curves for I_{peak} and I_{ss} in mouse apex myocytes ($n = 12$) under isosmotic, hyposmotic and hyperosmotic conditions. I_{peak} was measured as the peak of outward currents (at 10–50 ms) and I_{ss} was measured at the end of 4.5-s voltage steps. * $P < 0.05$, * * $P < 0.01$ *versus* isosmotic conditions.

densities of I_{ss} were 5.6 ± 0.5, 5.8 ± 0.5 and 5.4 ± 0.4 pA pF^{-1} under isosmotic, hyposmotic and hyperosmotic conditions, respectively ($n = 12$, NS).

Effects of hyposmotic cell swelling on $I_{to,fast}$ in mouse left ventricular apex myocytes

In mouse left ventricular apex, voltage-dependent outward K^+ currents are composed of at least four K^+ currents: $I_{to,fast}$, $I_{K,slow1}$, $I_{K,slow2}$ and I_{ss} (Xu *et al.* 1999*b*; Zhou *et al.* 2003). While $I_{K,slow2}$ can be selectively eliminated by 10 mM of TEA (Zhou *et al.* 2003), the separation of $I_{to,fast}$ from $I_{K,slow1}$ and I_{ss} was relatively more difficult. In this study, we adapted an approach established by Brouillette and colleagues to further effectively separate $I_{to,fast}$ from $I_{K,slow1}$ and I_{ss} in mouse ventricular myocytes (Brouillette *et al.* 2004). Because $I_{to,fast}$ inactivates much more rapidly than the other outward K^+ current components ($I_{K,slow1}$ and I_{ss}), it could be separated from those K^+ currents by using 'inactivating' prepulses (Fig. 3*A* and *B*) (Brouillette *et al.* 2004). In our experimental conditions $I_{to,fast}$ in mouse left ventricular apex myocytes inactivated completely at membrane potentials more positive than −20 mV (see Fig. 4). The time constant of $I_{to,fast}$ inactivation was 31 ± 7 ms (at +10 mV, $n = 7$). In addition, previous studies have shown that 10–100 μM of 4-AP can selectively block $I_{K,slow1}$ without significant effects on $I_{to,fast}$ in mouse ventricular myocytes (Xu *et al.* 1999*b*; Brouillette *et al.* 2004). In the present study, we also performed additional experiments with different concentrations of 4-AP (10, 50 and 100 μM) under isosmotic and hyposmotic conditions and found that 50 μM 4-AP was able to selectively block $I_{K,slow1}$ with insignificant blocking effects on $I_{to,fast}$ (see Fig. 3*A*). The osmotic challenge does not change the concentration–effect curves of 4-AP. Therefore, a combination of a 100-ms 'inactivating' prepulse to −20 mV and 50 μM of 4-AP in the bath solutions was used to effectively separate $I_{to,fast}$ from other K^+ currents in the ventricular myocytes.

Figure 3*Ab* shows the currents recorded by a depolarizing step from a 100-ms 'inactivating' prepulse of −20 mV to +10 mV for 500 ms in the presence of 50 μM 4-AP under isosmotic (Iso, upper traces) and hyposmotic (Hypo, lower traces) conditions. Subtraction of the traces

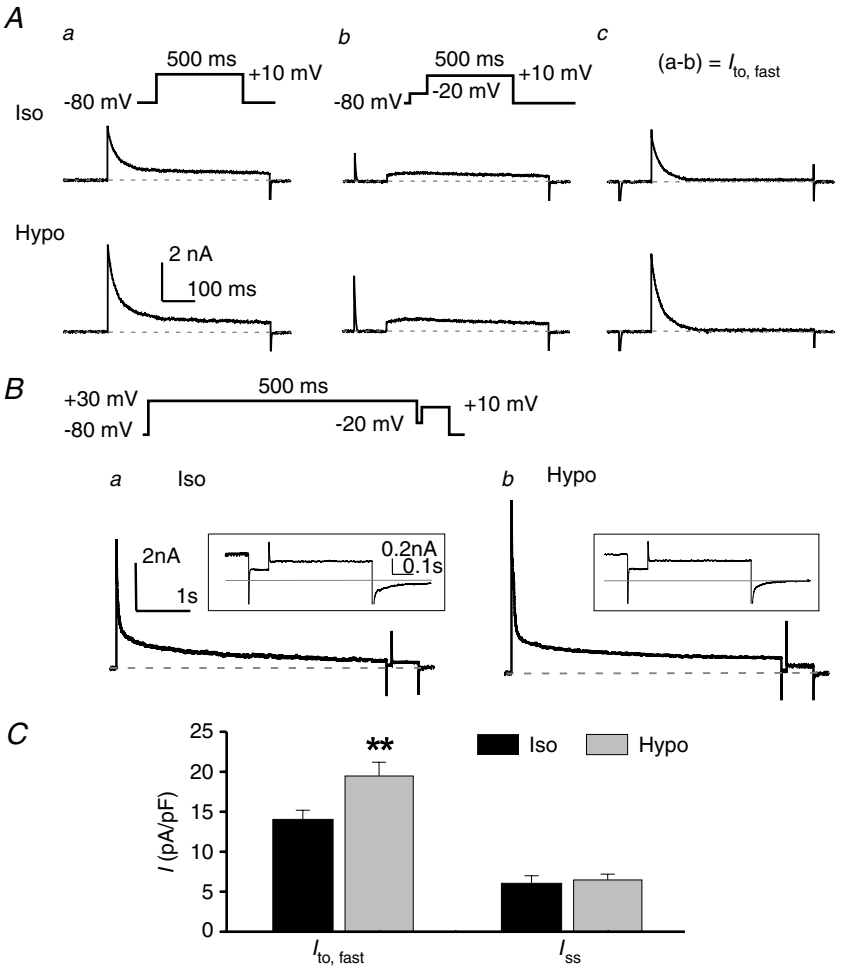

Figure 3. Hyposmotic cell swelling increases $I_{to,fast}$ but not I_{ss} in mouse left ventricular apex myocytes
A, effects of osmotic stress on $I_{to,fast}$. Whole-cell currents were recorded in the presence of 50 μM 4-AP from the same cell with voltage protocols shown on the top under isosmotic (Iso, upper traces) and hyposmotic (Hypo, lower traces) conditions. Cells were held at −80 mV, and currents were elicited by a 500-ms depolarizing voltage pulse to +10 mV (*a*) or by a 500-ms depolarizing step preceded by a 100-ms 'inactivating' prepulse to −20 mV to inactivate $I_{to,fast}$ (*b*). $I_{to,fast}$ was measured from the prepulse-sensitive difference currents obtained by subtracting the currents in panel *b* from the currents in panel *a* (*a* − *b*) under corresponding osmotic conditions (*c*). *B*, effects of hyposmotic cell swelling on I_{ss}. The voltage protocol (shown on the top) consists of a 5-s, +30-mV step and a 0.75-s, +10-mV step, which is interposed by a 100-ms 'inactivating' prepulse at −20 mV. The membrane currents elicited by the depolarization step from −20 mV to +10 mV are I_{ss}. Representative I_{ss} recorded under isosmotic (Iso) and hyposmotic (Hypo) conditions are shown on expanded time and current scales in panels *a* and *b*. The dashed lines indicate zero current. Representative whole-cell current traces are shown in the inset. *C*, mean current densities of $I_{to,fast}$ (*Ac*, $n = 7$) and I_{ss} (*B*, $n = 6$) in mouse left ventricular apex myocytes under isosmotic (black bars) and hyposmotic (grey bars) conditions. ** $P < 0.01$ *versus* isosmotic condition.

recorded with the inactivating prepulse protocol (Fig. 3*Ab*) from those without the prepulse (Fig. 3*Aa*) revealed a prepulse-sensitive current (Fig. 3*Ac*). This fast activating and inactivating prepulse-sensitive current corresponds to the $I_{to,fast}$ as previously described in mouse ventricular myocytes (Xu *et al.* 1999*b*; Brouillette *et al.* 2004). As shown in Fig. 3*Ac*, hyposmotic cell swelling significantly increased $I_{to,fast}$. The decaying phase of prepulse-sensitive current was well fitted by a single exponential function with mean values of the time constant of 27 ± 4 and 25 ± 3 ms under isosmotic and hyposmotic conditions, respectively ($n = 7$, $P > 0.05$), further confirming that this current is the fast inactivating $I_{to,fast}$. The inactivation kinetics of $I_{to,fast}$ was not affected by cell swelling.

The results shown in Figs 2 and 3*A* indicate that $I_{to,fast}$, but not I_{ss}, was regulated by hyposmotic cell swelling or hyperosmotic cell shrinkage. To further confirm this, as shown in Fig. 3*B*, a combination of 50 μM 4-AP and an inactivating prepulse (Fig. 3*B*, inset on top) was used to separate I_{ss} from $I_{K,slow1}$ and $I_{to,fast}$, respectively. The voltage protocol involves a long depolarizing voltage step from a holding potential of -80 mV to $+30$ mV for 5 s, which is sufficient to completely inactivate $I_{K,slow1}$ (Wang *et al.* 1999; Xu *et al.* 1999*b*; Brouillette *et al.*

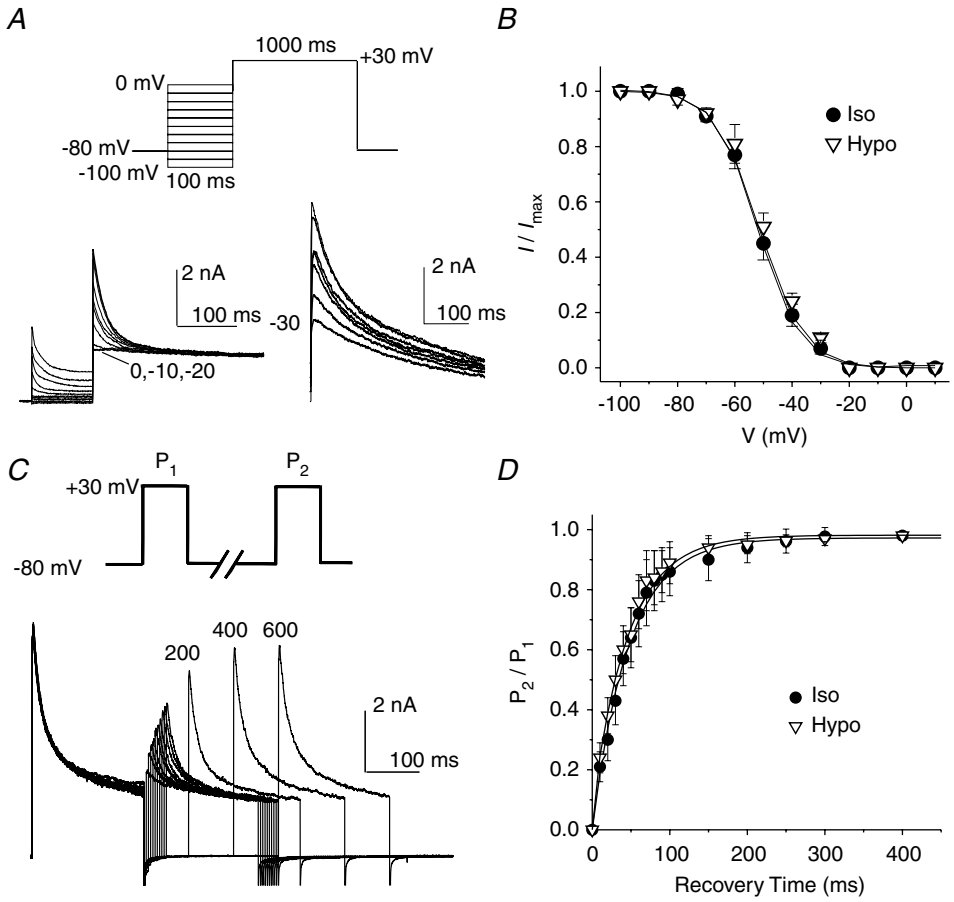

Figure 4. Effects of osmotic stress on voltage-dependent gating properties of $I_{to,fast}$ in mouse ventricular apex myocytes

A, the voltage dependence of steady-state inactivation of $I_{to,fast}$. Outward K^+ currents were recorded during 1-s depolarization to +30 mV after 100-ms prepulses to potentials between -100 and 0 mV (protocol shown on the top) in the presence of 50 μM 4-AP. The representative current traces recorded under hyposmotic conditions are shown on the left. The test pulse currents obtained with the -20, -10 and 0 mV prepulses were superimposed on each other. The difference currents were obtained by subtraction of the test pulse currents recorded with the -20-mV prepulse from those recorded with prepulses between -100 and 0 mV. No inactivating component was observed with prepulses of -20, -10 and 0 mV. Numbers next to current traces indicate the corresponding potential of the inactivating prepulse. *B*, mean steady-state voltage-dependent inactivation curve of $I_{to,fast}$ under isosmotic and hyposmotic conditions ($n = 6$). Peak $I_{to,fast}$ recorded at +30 mV was normalized to the corresponding current amplitude measured at -100 mV. *C* and *D*, effects of cell swelling on the recovery from inactivation of $I_{to,fast}$; *C*, representative current traces recorded using a double-pulse voltage protocol (shown on the top); D, recovery of $I_{to,fast}$ from inactivation under isosmotic and hyposmotic conditions ($n = 7$).

2004), followed by a brief 100-ms 'gap' at −20 mV, which inactivates $I_{to,fast}$. The current activated by the second depolarizing step from −20 mV to +10 mV for 750 ms was the non-inactivating current I_{ss} as shown with expanded time and current scales in the insets. The amplitude of I_{ss} under isosmotic conditions (Fig. 3*Ba*) was unchanged after exposure to hyposmotic solutions (Fig. 3*Bb*). Similar results were observed when the same voltage protocol was applied to the same cells in the absence of 50 μM 4-AP (data not shown). Figure 3*C* summarizes the mean current densities of $I_{to,fast}$ (as measured in Fig. 3*Ac*) and I_{ss} (as measured in Fig. 3*Ba* and *b*) obtained under isosmotic (black bars) and hyposmotic (grey bars) conditions, respectively. Consistent with previous reports (Xu *et al.* 1999*b*), $I_{to,fast}$ is a major contributor to the peak outward K^+ currents under both osmotic conditions, while I_{ss} was significantly smaller than $I_{to,fast}$. The current density of $I_{to,fast}$ was significantly increased from 14.1 ± 1.1 to 19.5 ± 1.5 pA pF^{-1} ($n = 7$, $P < 0.01$) by hyposmotic cell swelling, whereas the current density of I_{ss} was not changed after exposure to hyposmotic solution (6.1 ± 0.9 and 6.5 ± 0.7 pA pF^{-1} under isosmotic and hyposmotic conditions, respectively; $n = 6$, $P > 0.05$). When hyperosmotic perfusion was applied to the cells first, there was a significant decrease in the current amplitude of $I_{to,fast}$ in mouse ventricular myocytes. For example, the mean current density of $I_{to,fast}$ at +10 mV was decreased from 15.2 ± 1.2 to 10.5 ± 1.5 pA pF^{-1} ($n = 4$, $P < 0.01$) by hyperosmotic cell shrinkage.

The above results indicate that: (1) $I_{to,fast}$ in native mouse ventricular myocytes can be effectively separated from other outward K^+ current components ($I_{K,slow1}$ and I_{ss}) using a combination of voltage protocols and pharmacological tools; (2) hyposmotic cell swelling activates $I_{to,fast}$ but not I_{ss}, suggesting that specific activation of $I_{to,fast}$ may be responsible for the shortening in early repolarization (APD_5 and APD_{10}).

Effects of hyposmotic cell swelling on voltage-dependent gating properties of $I_{to,fast}$

We next tested whether the regulation of $I_{to,fast}$ by cell volume changes is due to changes in the voltage-dependent gating mechanism. The steady-state voltage-dependent inactivation of $I_{to,fast}$ was examined using the double-pulse protocol (see Methods) in the presence of 50 μM 4-AP as previously described (Brouillette *et al.* 2004), under isosmotic and hyposmotic conditions (Fig. 4*A*). As shown by the current traces on the left in Fig. 4*A*, the test pulse currents obtained with inactivating prepulses of 0, −10 and −20 mV were superimposed. The current traces on the right in Fig. 4*A* were the difference currents obtained from the subtraction of the currents recorded with the prepulse of −20 mV from those with prepulses from −100 to 0 mV. No inactivating components were observed at prepulses of −20, −10 and 0 mV, indicating that $I_{to,fast}$ could be inactivated completely at a membrane voltage more positive than −20 mV. These results also confirm that it is optimal to choose −20 mV as the inactivating prepulse for separation of $I_{to,fast}$. Figure 4*B* shows the mean steady-state inactivation curve of $I_{to,fast}$ averaged from six cells. Consistent with previous observations in mouse ventricular myocytes (Xu *et al.* 1999*b*; Brouillette *et al.* 2004), the steady-state inactivation of $I_{to,fast}$ was best fitted by a single Boltzmann function with a derived $V_{1/2}$ of -48.5 ± 0.6 mV and slope factor (k) of 7.7 ± 0.4 mV under isosmotic conditions. Hyposmotic cell swelling failed to alter both parameters (-49.7 ± 1.3 and 7.0 ± 0.4 mV, respectively; $n = 6$, $P > 0.05$).

The process of $I_{to,fast}$ recovery from inactivation under isosmotic and hyposmotic conditions was examined using a double-pulse protocol in the presence of 50 μM 4-AP (see Methods) (Brouillette *et al.* 2004). Figure 4*C* shows representative current traces recorded under hyposmotic conditions. Figure 4*D* summarizes the time course of recovery of $I_{to,fast}$ from inactivation. Under isosmotic conditions the recovery process of $I_{to,fast}$ was best fitted by a single exponential function with a mean time constant (τ) of 49 ± 6 ms. Exposure to hyposmotic solutions failed to significantly alter the recovery process ($\tau = 46 \pm 7$ ms, $n = 7$, $P > 0.05$). Since the recovery of $I_{to,fast}$ from inactivation is a voltage-dependent process (Brouillette *et al.* 2004) we further examined whether osmotic challenge affects the kinetics of recovery from inactivation at different holding potentials. The recovery of $I_{to,fast}$ was significantly faster at more hyperpolarized potentials under isosmotic conditions. The mean time constants (τ) were 49 ± 6, 68 ± 5 and 127 ± 6 ms ($n = 7$) at −80, −70 and −60 mV, respectively. No significant changes in the recovery process were observed when the cells were exposed to hyposmotic solutions. The corresponding mean τ values were 46 ± 7, 64 ± 7 and 119 ± 8 ms at holding potentials of −80, −70 and −60 mV, respectively ($n = 7$, $P > 0.05$).

Taken together, these results indicate that cell swelling increased $I_{to,fast}$ current density through a mechanism that was independent of the voltage-gating properties of the channel.

Role of PKC and phosphatases in the regulation of $I_{to,fast}$ by hyposmotic cell swelling

As described above in Fig. 2*A*, the onset of changes in $I_{to,fast}$ was slower than changes in the cell volume, suggesting that an intracellular signalling transduction pathway may be involved in the volume regulation of the channels. Indeed, numerous previous studies have reported that changes in protein phosphorylation/dephosphorylation activities are

closely related to changes in cell volume in a variety of cell types of different species (for review see Duan *et al.* 1999*a*; Lang *et al.* 2000; Zhong *et al.* 2002; Baumgarten & Clemo, 2003). In some cells, including cardiac cells, hyposmotic cell swelling induces protein dephosphorylation whereas cell shrinkage causes protein phosphorylation due to altered activities of protein kinases and/or phosphatases (Duan *et al.* 1995, 1999*a*; Duan & Hume, 2000; Ellershaw *et al.* 2000; Lang *et al.* 2000; Rutledge *et al.* 2001; Zhong *et al.* 2002; Ellershaw *et al.* 2002). In cardiac and many non-cardiac cells, for example, volume regulation of Cl^- channels is linked to PKC phosphorylation and dephosphorylation (Duan *et al.* 1995, 1999*a*; Lang *et al.* 2000; Ellershaw *et al.* 2002; Zhong *et al.* 2002; Baumgarten & Clemo, 2003). It is noteworthy that both native I_{to} in cardiac myocytes and the expressed $K_v4.2$ and $K_v4.3$ currents have been previously reported to be regulated by PKC (Nakamura *et al.* 1997; Po *et al.* 2001; Shimoni & Liu, 2003) or protein phosphatases (Caballero *et al.* 2004). Therefore, we tested whether volume regulation of native $I_{to,fast}$ in mouse heart is also mediated through a phosphorylation/dephosphorylation mechanism.

Figure 5 shows the effects of a PKC activator, phorbol-12,13-dibutyrate (PDBu, 100 nM), on $I_{to,fast}$ in mouse left ventricular apex myocytes. As described above in Fig. 3*A*, $I_{to,fast}$ was measured by subtracting the current recorded with an inactivating prepulse

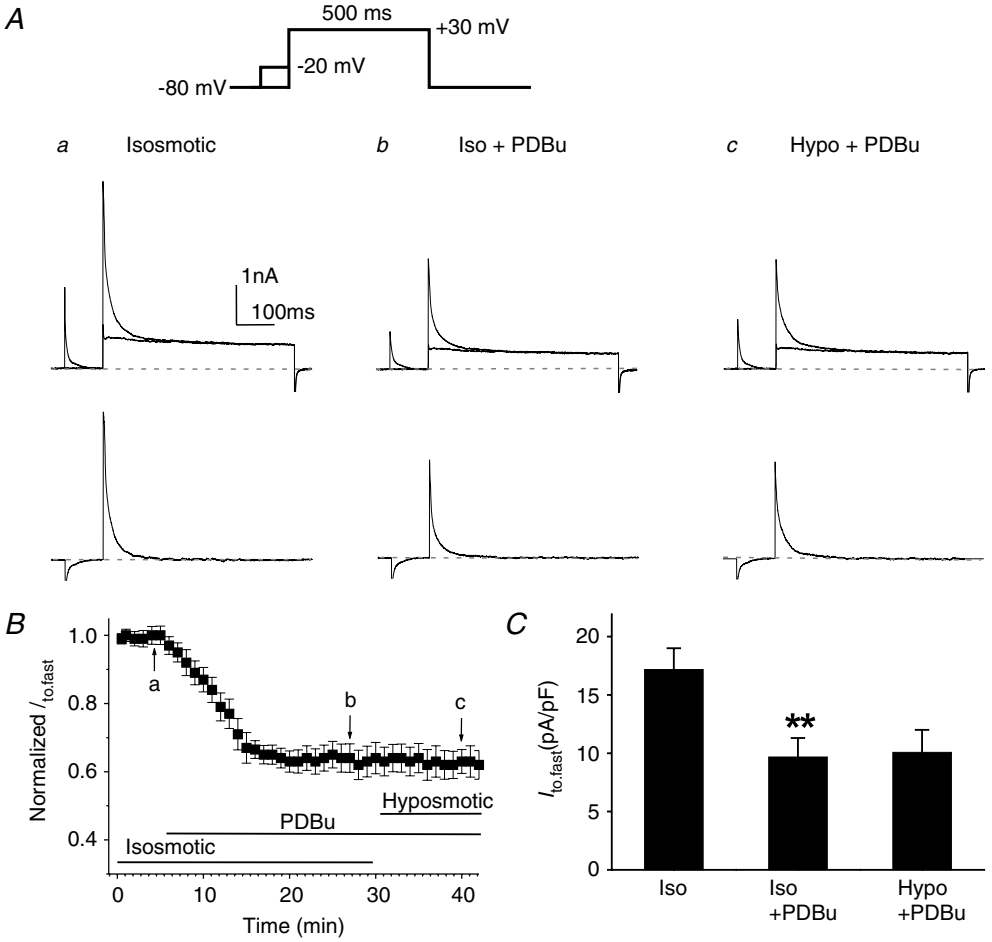

Figure 5. Effects of PKC activator (PDBu) on $I_{to,fast}$ in mouse left ventricular apex myocytes
A, representative current traces of $I_{to,fast}$ (lower traces in each panel) obtained from the subtraction of currents recorded with the inactivating prepulse from those recorded without the inactivating prepulse (upper superimposed traces) in the presence of 50 μM 4-AP. Voltage protocols are shown on the top. The same cell was consecutively exposed to isosmotic solution (*a*), isosmotic + PDBu (100 nM, *b*), and hyposmotic + PDBu (100 nM, *c*). PDBu decreased $I_{to,fast}$ under isosmotic conditions and subsequent hyposmotic perfusion failed to further activate $I_{to,fast}$. *B*, time course of changes in normalized $I_{to,fast}$ at +30 mV when cells were exposed consecutively to isosmotic, isosmotic + PDBu, and hyposmotic + PDBu solutions. Peak $I_{to,fast}$ was recorded every 1 min then normalized to the initial corresponding value at time 0 ($n = 7$). *C*, mean peak current densities of $I_{to,fast}$ recorded when cells were exposed to isosmotic, isosmotic + PDBu, and hyposmotic + PDBu solutions. Currents were obtained using the protocols shown in panel *A* ($n = 7$). $^{**}P < 0.01$ *versus* isosmotic (Iso) condition.

at −20 mV for 100 ms from that recorded without the prepulse in the presence of 50 μM 4-AP. In Fig. 5*A*, the representative current traces recorded with and without the prepulses are superimposed (upper traces). The corresponding difference currents ($I_{to,fast}$) yielded from the subtraction under isosmotic (*a*), isosmotic + PDBu (*b*) and hyposmotic + PDBu (*c*) conditions are shown in the lower panels. When the cells were exposed to isosmotic solutions for 5 min, activation of PKC by PDBu caused a time-dependent inhibition of the peak $I_{to,fast}$, which reached the steady state within 10 min. Subsequent exposure of the cells to hyposmotic solutions in the presence of PDBu failed to increase $I_{to,fast}$ (Fig. 5*B*). Similar results were observed in seven cells. At +30 mV, for example, PDBu significantly inhibited $I_{to,fast}$ (from 17.2 ± 1.8 to 9.7 ± 1.6 pA pF^{-1}, $n = 7$, $P < 0.01$) under isosmotic conditions and prevented further activation by hyposmotic cell swelling (10.1 ± 1.9 pA pF^{-1}, $n = 7$, $P > 0.05$). The mean current densities of $I_{to,fast}$ recorded at +30 mV under corresponding conditions to those in Fig. 5*A* and *B* are shown in Fig. 5*C*. When cells were treated with 100 nM 4α-phorbol 12, 13-didecanoate (4α-PDD; an inactive form of PDBu), however, no inhibition of $I_{to,fast}$ by 4α-PDD was observed and hyposmotic cell swelling caused a similar increase in $I_{to,fast}$ as seen in the absence of either 4α-PDD or PDBu (data not shown); this suggests that the observed effect of PDBu on volume regulation of $I_{to,fast}$ is not due to a non-specific effect of phorbol esters.

To further test whether PKC is indeed involved in the volume regulation of $I_{to,fast}$ in cardiac myocytes, we examined the effect of a PKC inhibitor, bisindolylmaleimide (BIM; 100 nM), on cell volume regulation of $I_{to,fast}$. As shown in Fig. 6, exposure of the cells to BIM under isosmotic condition caused

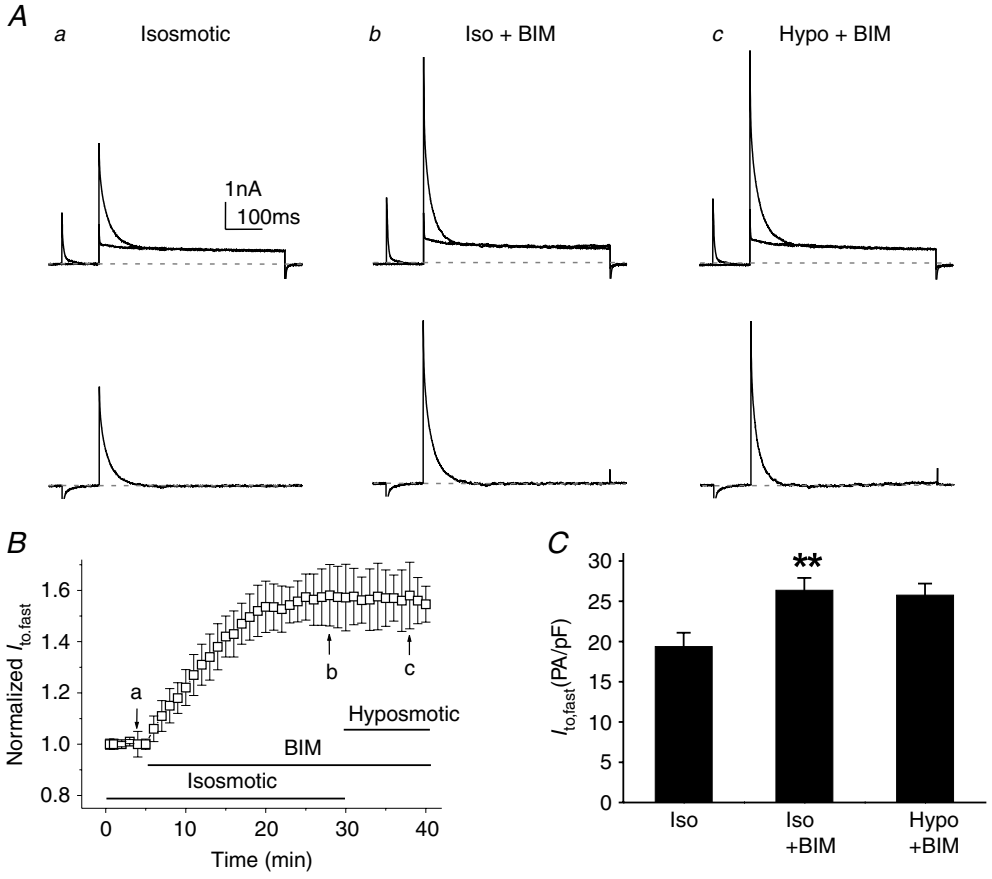

Figure 6. Effects of PKC inhibitor (BIM) on $I_{to,fast}$ in mouse left ventricular apex myocytes
A, representative current traces of $I_{to,fast}$ recorded from a ventricular myocyte using the same voltage protocols as shown in Fig. 5*A* in the presence of 50 μM 4-AP when the same cell was consecutively exposed to isosmotic (*a*), isosmotic + BIM (100 nM, *b*), and hyposmotic + BIM (*c*) solutions. *B*. time course of changes in normalized $I_{to,fast}$ at +30 mV when cells were exposed consecutively to isosmotic, isosmotic + BIM, and hyposmotic + BIM solutions. The amplitudes of $I_{to,fast}$ were recorded every 1 min and then normalized to the initial corresponding value at time 0 ($n = 7$). *C*, mean peak current densities of $I_{to,fast}$ ($n = 7$) recorded at +30 mV when cells were exposed to isosmotic, isosmotic + BIM (Iso + BIM), and hyposmotic + BIM (Hypo + BIM) solutions using protocols shown in Fig. 5*A*. $^{**}P < 0.01$ *versus* isosmotic (Iso) conditions.

a significant increase in $I_{to,fast}$ in a time-dependent fashion (Fig. 6*B*). At +30 mV, $I_{to,fast}$ was increased from 19.4 ± 1.7 to 26.4 ± 1.5 pA pF^{-1} ($n = 6$, $P < 0.01$) and reached the steady state within 20 min. In the presence of BIM, however, hyposmotic cell swelling failed to further increase $I_{to,fast}$ (25.8 ± 1.4 pA pF^{-1}, $n = 7$, $P > 0.05$ *versus* isosmotic + BIM) (Fig. 6*C*). These results suggest that cell volume regulation of $I_{to,fast}$ in mouse ventricular myocytes may be linked to a PKC-mediated phosphorylation and dephosphorylation activity.

In intact cells, protein phosphorylation processes are reversibly controlled by protein kinases and protein phosphatases (Hunter, 1995; Herzig & Neumann, 2000). The balance of kinase and phosphatase activities directly determines the net level of protein phosphorylation (Cohen, 1992). Both protein kinases and phosphatases have been reported to be subject to regulation by cell volume (Jennings & Schulz, 1991; Lang *et al.* 1998; Duan *et al.* 1999*a*). To further test the hypothesis that a balance between channel protein phosphorylation and dephosphorylation may be the key regulatory event responsible for $I_{to,fast}$ regulation by cell volume in the face of osmotic perturbation, we studied the effects of two highly potent serine/threonine protein phosphatase inhibitors: okadaic acid (Cohen, 1992; Duan *et al.* 1999*a*) and calyculin A (Ishihara *et al.* 1989; Duan *et al.* 1999*a*), on the osmotic regulation of mouse ventricular $I_{to,fast}$. As shown in Fig. 7*A*, the current amplitude of $I_{to,fast}$ started to decrease after the cell was exposed to okadaic acid (OA; 100 nM) for >2 min in the isosmotic bath solution and reached the steady-state level after ~25 min (Fig. 7*Ab*). In the presence of OA, subsequent exposure of the cell to hyposmotic solution for 10 min caused no changes in $I_{to,fast}$ (Fig. 7*Ac*). Washout of OA with hyposmotic bath solution for >10 min increased $I_{to,fast}$ (Fig. 7*Ad*). Re-application of OA in the same hyposmotic solution inhibited $I_{to,fast}$ again. Figure 7*B* summarizes the relationship between changes in mean $I_{to,fast}$ current densities and cell volume of six different mouse ventricular myocytes under isosmotic, isosmotic + OA, hyposmotic + OA, and hyposmotic conditions. Under isosmotic conditions, exposure of the cells to OA caused a significant decrease (from 17.1 ± 1.5 to 11.5 ± 1.4 pA pF^{-1}, $n = 6$, $P < 0.05$) in $I_{to,fast}$ but no significant changes in cell volume ($12\,032 \pm 1671$ μm^3 *versus* $11\,274 \pm 1816$ μm^3, $n = 6$, $P > 0.05$). In the presence of OA, subsequent exposure of the cells to hyposmotic solution caused a significant increase in cell volume ($20\,416 \pm 2174$ μm^3, $n = 6$, $P < 0.05$) but no further significant changes in $I_{to,fast}$ (11.2 ± 1.8 pA pF^{-1}, $n = 6$, NS). Washout of OA with hyposmotic solution, however, caused a significant increase in $I_{to,fast}$ (23.3 ± 1.6 pA pF^{-1}, $n = 6$, $P < 0.05$) while the cell volume remained almost unchanged ($20\,145 \pm 2786$ μm^3, $P > 0.05$). Similar results were also observed when another more potent phosphatase inhibitor, calyculin A (CA, 20 nM), was used under identical conditions to those described above for OA (Fig. 7*C*). These data strongly indicate that inhibition of serine/thronine phosphatases (types 1 and 2A; PP1 and PP2A) not only inhibited $I_{to,fast}$ but also prevented the effect of hyposmotic cell swelling on the channel in the intact cardiac myocytes.

Taken together, these results indicate that phosphorylation of the channel, by either increase in the protein kinase activity or decrease in the phosphatase activity, caused an inhibition of the channel activity; dephosphorylation of the channel, by increase in the phosphatase activity or decrease in the protein kinase activity, caused an activation of the channels; these results suggest that the balance of PKC–phosphatase activity may be constantly regulated by cell volume and may be the key regulatory process responsible for the regulation of $I_{to,fast}$ by cell volume in the face of osmotic challenges.

Volume regulation of $K_v4.2$ and $K_v4.3$ channels expressed in NIH/3T3 cells

To further investigate the molecular mechanism underlying the volume regulation of $I_{to,fast}$ in cardiac myocytes, we examined whether cell volume changes also regulate $K_v4.2$ and $K_v4.3$ channels since the primary subunits that contribute to $I_{to,fast}$ are the $K_v4.2$ or $K_v4.3$ channels, or a combination of the two (Dixon *et al.* 1996; Johns *et al.* 1997; Hoppe *et al.* 2000).

As shown in Fig. 8*A*, expression of $K_v4.2$ in NIH/3T3 cells yielded large transient outward currents when the cells were depolarized from a holding potential of −80 mV to a variety membrane potentials in increments of +10 mV under isosmotic conditions (Fig. 8*Aa*); in contrast, only very small endogenous voltage-gated outward currents were recorded from untransfected cells (data not shown). The expressed $K_v4.2$ currents were markedly blocked by 5 mM 4-AP (data not shown). These results are consistent with previous studies from other investigators (Ohya *et al.* 1997; Hatano *et al.* 2003). Exposure of the cells to hyposmotic solutions increased $K_v4.2$ currents (Fig. 8*Ab*) and subsequent exposure to hyperosmotic solutions decreased the currents (Fig. 8*Ac*). Similar results were observed in 12 cells under identical conditions and the mean *I–V* curves of the $K_v4.2$ currents under isosmotic, hyposmotic and hyperosmotic conditions are shown in Fig. 8*B* ($n = 12$). The mean current density of $K_v4.2$ channels was increased significantly by hyposmotic swelling over the range −10 to +60 mV, switch from hyposmotic perfusion to hyperosmotic perfusion decreased the current amplitude significantly over the range 0 to +60 mV. Consistent with observations in the endogenous $I_{to,fast}$ in native cardiac myocytes (Fig. 4), no significant effects of osmotic stress on the voltage dependence of steady-state inactivation of $K_v4.2$ channels

were observed (Fig. 8*C*). The $V_{1/2}$ values of $K_v4.2$ channels were -36.6 ± 0.6, -34.7 ± 0.5 and -33.9 ± 1.2 mV and k values of $K_v4.2$ channels were -6.3 ± 0.2, -7.7 ± 0.6, and -7.7 ± 0.3 mV under isosmotic, hyposmotic and hyperosmotic conditions, respectively ($n = 6$, $P > 0.05$). As shown in Fig. 8*D*, the recovery kinetics of $K_v4.2$ channels was not significantly altered by cell volume changes. The time constants (τ) were 303 ± 43, 317 ± 41

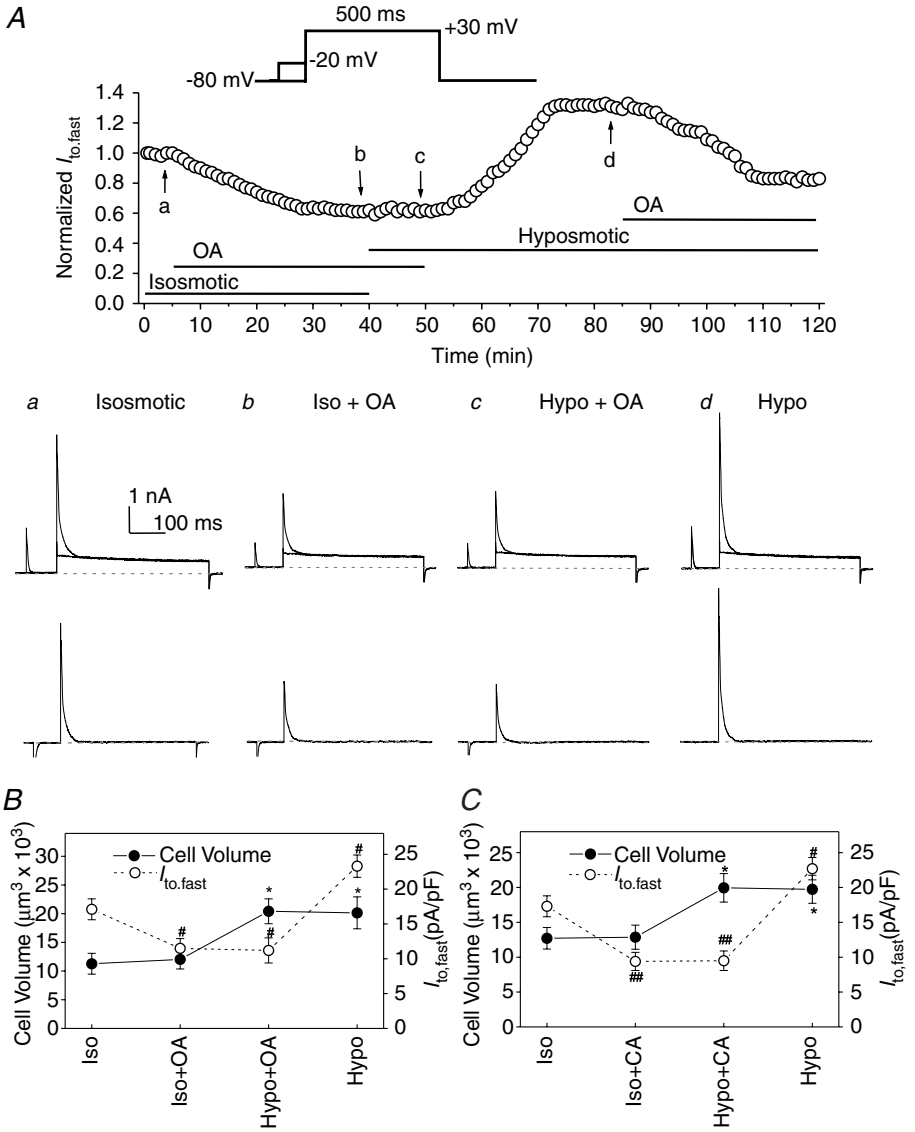

Figure 7. Effects of serine/threonine protein phosphatase inhibitors, okadaic acid and calyculin A, on $I_{to,fast}$ in mouse left ventricular myocytes

A, whole-cell currents were monitored continuously in the presence of 50 μM 4-AP (voltage-clamp protocols shown on the top, also see Fig. 3*A* for details). Top panel, $I_{to,fast}$ was recorded every 1 min then normalized to the initial corresponding value at time 0 when cardiac myocytes were consecutively exposed to isosmotic, isosmotic + OA (100 nM), hyposmotic + OA (100 nM), and hyposmotic solutions. Changes in perfusion solutions were started when the changes in current amplitude reached the steady-state level. *a–d*, the representative superimposed current traces (upper) and the prepulse-sensitive difference current ($I_{to,fast}$) traces (lower) recorded from the same cell as shown in the top panel at the time points indicated by the arrows. *B*, changes in mean peak $I_{to,fast}$ current densities (○, *y*-axis on the left) and cell volume (●, *y*-axis on the right) recorded when cells were consecutively exposed to isosmotic (Iso), isosmotic +100 nM OA (Iso + OA), hyposmotic +100 nM OA (Hypo + OA), and hyposmotic (Hypo) solutions ($n = 6$). Currents were obtained using the protocols described in panel *A* ($^*P < 0.05$ when compared with cell volume under control (Iso) conditions; $^{\#}P < 0.05$ when compared with peak current density under control (Iso) conditions). *C*, changes in mean peak $I_{to,fast}$ current densities (○) and cell volume (●) recorded from cardiac myocytes when they were consecutively exposed to isosmotic (Iso), isosmotic + 20 nM CA (Iso + CA), hyposmotic + 20 nM CA (Hypo + CA), and hyposmotic (Hypo) solutions ($n = 5$, $^*P < 0.05$ when compared with cell volume under control (Iso) conditions; $^{\#}P < 0.05$, $^{\#\#}P < 0.01$ when compared with peak current density under control (Iso) conditions).

and 291 ± 38 ms under isosmotic, hyposmotic and hyperosmotic conditions, respectively ($n = 7$, NS).

Similarly, $K_v4.3$ channels expressed in NIH/3T3 cells were also regulated by changes in cell volume. When measured at +40 mV, for example, exposure of the cells to hyposmotic solutions increased $K_v4.3$ current density from 44.5 ± 3.4 to 72.2 ± 9.1 pA pF^{-1} ($n = 10$, $P < 0.01$), and subsequent exposure to hyperosmotic solutions decreased $K_v4.3$ current density to 39.0 ± 3.2 pA pF^{-1} ($P < 0.01$). Consistent with the observations in native $I_{to,fast}$ and expressed $K_v4.2$ channels, neither the voltage-dependent inactivation nor the recovery from inactivation of the expressed $K_v4.3$ channels were altered by cell volume changes (data not shown).

Role of PKC and phosphatases in cell volume regulation of $K_v4.2$ and $K_v4.3$ channels

We further examined the effects of PKC activator (PDBu), PKC inhibitor (BIM), and phosphatase inhibitors (OA and CA) on volume regulation of $K_v4.2$ and $K_v4.3$ channels under the same conditions as described for endogenous $I_{to,fast}$ in native mouse cardiac myocytes. As shown in Fig. 9*A*, PDBu (100 nM) caused a time-dependent inhibition of $K_v4.2$ currents under isosmotic conditions and prevented the activation of the current by hyposmotic cell swelling (Fig. 9*Aa*). Similar results were observed in six different cells. The mean *I–V* curves under isosmotic, isosmotic + PDBu, and hyposmotic + PDBu are summarized in Fig. 9*Ab*. Similar results were also

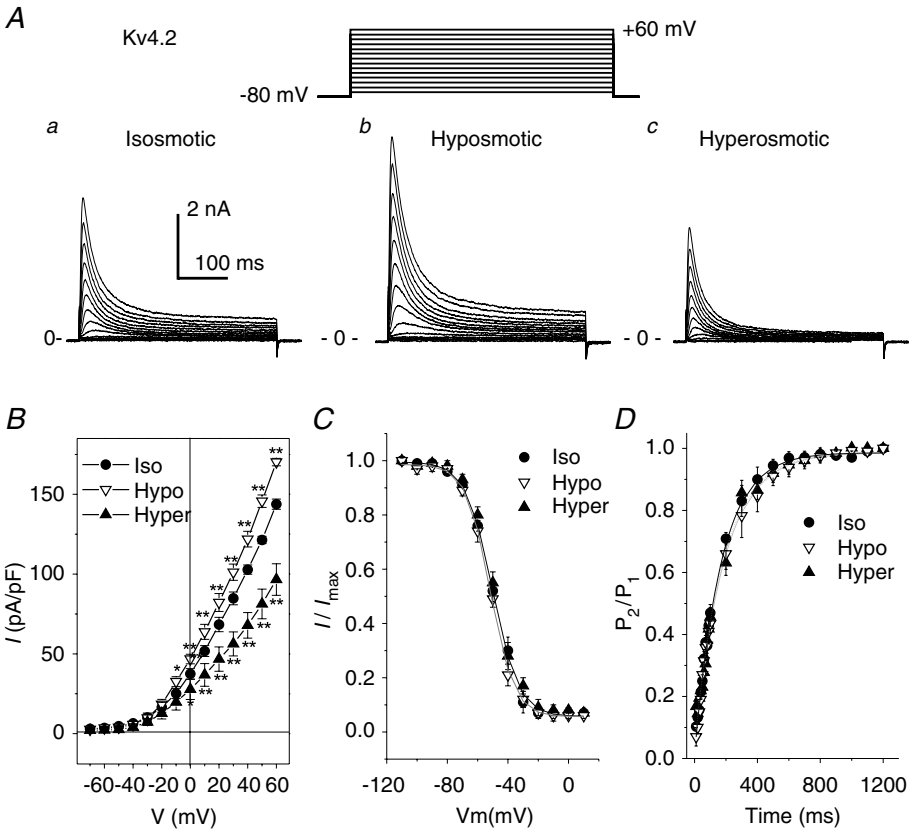

Figure 8. Effects of osmotic stress on $K_v4.2$ channels in NIH/3T3 cells
A, representative whole-cell currents recorded from NIH/3T3 cells expressing the rat $K_v4.2$ gene under isosmotic (*a*), hyposmotic (*b*) and hyperosmotic (*c*) conditions. $K_v4.2$ currents were elicited by a series of 400-ms depolarizing voltage steps (inset). *B*, mean *I–V* curves of $K_v4.2$ channels ($n = 12$) recorded under isosmotic, hyposmotic and hyperosmotic conditions. *C*, mean steady-state voltage-dependent inactivation curves of $K_v4.2$ ($n = 6$) obtained from a double-pulse protocol (inset in *A*,) under isosmotic, hyposmotic and hyperosmotic conditions. *D*, recovery from inactivation was examined using a double-pulse protocol with different recovery times (see Methods). Mean normalized currents ($n = 7$) under isosmotic, hyposmotic and hyperosmotic conditions were plotted against recovery time. The kinetics of recovery from inactivation was a single exponential process (continuous lines) with a time constant (τ) of 303 ± 43, 317 ± 41 and 291 ± 38 ms ($P > 0.05$) under isosmotic, hyposmotic and hyperosmotic conditions, respectively.

observed in the $K_v4.3$ channels expressed in NIH/3T3 cells. Activation of PKC by PDBu reduced $K_v4.3$ currents from 47.4 ± 2.5 to 32.0 ± 3.3 pA pF^{-1} at +40 mV ($n = 7$, $P < 0.05$) under isosmotic conditions. No further increase in $K_v4.3$ currents was observed (34.5 ± 3.7 pA pF^{-1}, $P > 0.05$) when cells were exposed to hyposmotic solution in the presence of PDBu.

When the cells were exposed to BIM (100 nM), on the other hand, a time-dependent increase in peak $K_v4.2$ current between +10 mV and 60 mV was observed (Fig. 9*B*). The peak $K_v4.2$ current densities at +40 mV were increased from 103.9 ± 4.5 to 125.1 ± 4.6 pA pF^{-1} ($n = 5$, $P < 0.01$). In the presence of BIM, no further increase in $K_v4.2$ currents was observed when the cells were perfused with hyposmotic solutions for >10 min (122.3 ± 3.7 pA pF^{-1} at +40 mV, $P > 0.05$). The mean *I–V* curves recorded from five different cells under isosmotic, isosmotic + BIM, and hyposmotic + BIM conditions are summarized in Fig. 9*Bb*. Similarly, inhibition of PKC by BIM also increased $K_v4.3$ currents at +40 mV from 44.2 ± 3.5 to 61.7 ± 3.3 pA pF^{-1} ($n = 6$, $P < 0.01$) under isosmotic conditions. Subsequent hyposmotic cell swelling in the presence of BIM failed to further increase the current (63.5 ± 4.2 pA pF^{-1}, $n = 6$, $P > 0.05$).

As shown in Fig. 10, both OA (Fig. 10*A*) and CA (Fig. 10*B*) caused a time-dependent inhibition of $K_v4.2$ currents under isosmotic conditions and prevented further activation of the currents by hyposmotic cell swelling. Similar effects of OA and CA on the $K_v4.3$ channels expressed in NIH/3T3 cells were also observed. For example, under isosmotic conditions, OA (100 nM) reduced the current amplitude of $K_v4.3$ at +40 mV from 45.2 ± 3.1 to 33.1 ± 2.9 pA pF^{-1} ($n = 4$, $P < 0.05$) and no further increase in $K_v4.3$ currents was observed when cells were exposed to hyposmotic solutions in the presence of OA (35.7 ± 2.9 pA pF^{-1}, $n = 4$, NS). Similarly, CA (20 nM) reduced $K_v4.3$ current amplitude from 47.3 ± 2.8 to 36.1 ± 2.7 pA pF^{-1} ($n = 4$, $P < 0.05$) and no further increase in $K_v4.3$ currents was observed when cells were exposed to hyposmotic solutions in the presence of CA (36.3 ± 2.8 pA pF^{-1}, $n = 4$, $P > 0.05$).

Discussion

Our results provide the following evidence for a novel regulation mechanism for $K_v4.2/4.3$ K^+ channels in the heart: (1) $I_{to,fast}$ in native mouse left ventricular apex myocytes, and its key molecular counterparts

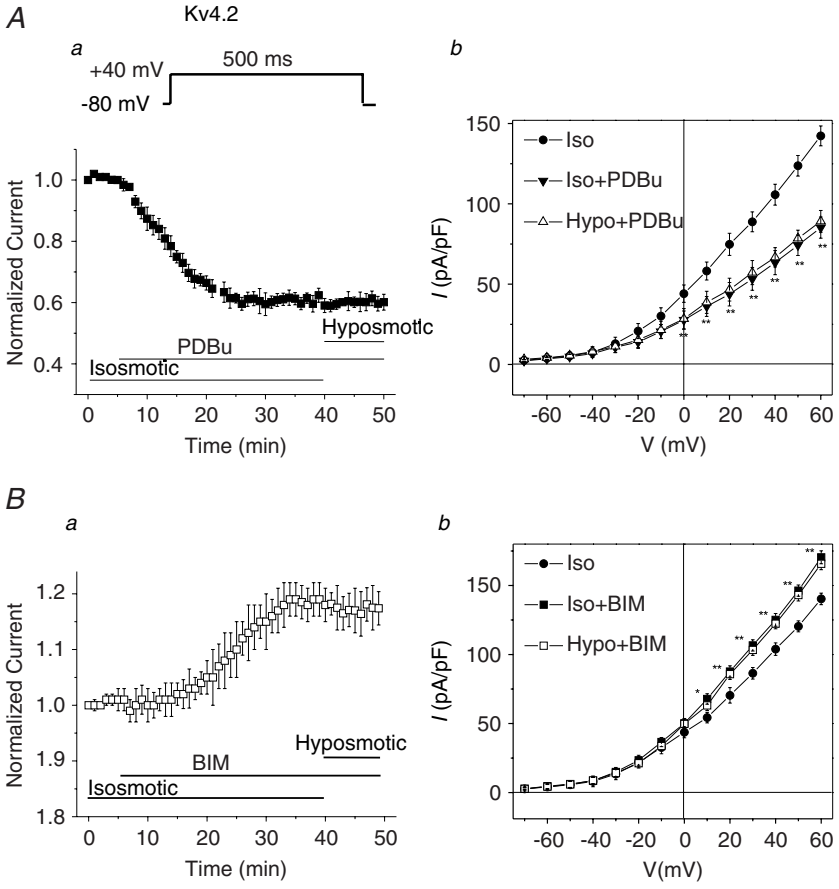

Figure 9. Effects of PKC activator (PDBu) and inhibitor (BIM) on $K_v4.2$ currents in NIH/3T3 cells
A, effect of PDBu (100 nM) on peak $K_v4.2$ currents. *a,* time course of changes in normalized peak $K_v4.2$ currents ($n = 6$) measured at +40 mV under isosmotic, isosmotic + PDBu, and hyposmotic + PDBu conditions. *b*, *I–V* curves of $K_v4.2$ channels ($n = 7$) recorded using a protocol as described in Fig. 5 in isosmotic (Iso), isosmotic + PDBu (Iso + PDBu), and hyposmotic + PDBu (Hypo + PDBu) solutions. PDBu inhibited the currents under isosmotic conditions and prevented further activation by hyposmotic cell swelling. *B*, effects of BIM on $K_v4.2$ channels. *a*, time course of changes in normalized peak $K_v4.2$ currents recorded at +40 mV under isosmotic, isosmotic + BIM, and hyposmotic + BIM conditions ($n = 5$). *b*, mean *I–V* curves of $K_v4.2$ channels ($n = 5$) in isosmotic (Iso), isosmotic + BIM (Iso + BIM), and hyposmotic + BIM (Hypo + BIM) solutions. BIM caused a time-dependent increase in $K_v4.2$ currents even under isosmotic conditions and prevented further activation by hyposmotic cell swelling.

K_v4.2/4.3 channels expressed in NIH/3T3 cells, are strongly regulated by cell volume changes which may be responsible for hyposmotic cell swelling-induced shortening in early repolarization of APD in cardiac myocytes; (2) changes in cell volume alter the amplitude of these currents with no effect on their voltage-dependent gating properties including activation, inactivation and recovery from inactivation; (3) cell volume regulation of these channels is closely coupled to a phosphorylation/dephosphorylation process mediated by PKC and serine/thronine phosphatases. These findings are potentially very important because the K_v4.2/4.3-encoded $I_{to,fast}$ plays a crucial role in APD repolarization and ECC in the heart, and changes in expression and function of K_v4.2/4.3 are regarded as hallmark features of diseased myocardium in human and numerous other animal models (Barry *et al.* 1998; Kaab *et al.* 1998; Wang *et al.* 1999; Yue *et al.* 1999; Huang *et al.* 2000).

Volume regulation of ion channels and adaptive remodelling of cardiac myocytes

Perturbations in cell volume and ion channel function are closely associated during adaptive structural and electrical remodelling of the cardiac myocytes such as hypertrophic cell volume increase caused by pressure overload or changes in extracellular osmolarity caused by myocardial hypoxia, ischaemia and reperfusion (Steenbergen *et al.* 1985; Wright & Rees, 1998; Befroy *et al.* 1999; Baumgarten & Clemo, 2003; Frey *et al.* 2004; Duan *et al.* 2005). It has been demonstrated that cardiac myocytes are able to avoid excessive cell volume changes through the regulation of loss or gain of intracellular ions or other osmolytes (Duan *et al.* 1999*a*; Hume *et al.* 2000; Lang *et al.* 2000; Baumgarten & Clemo, 2003). Several ionic mechanisms such as $I_{Cl,swell}$ (Duan *et al.* 1995, 1997*a*,*b*, 1999*a*; Vandenberg *et al.* 1997; Hiraoka *et al.* 1998), $I_{K,s}$ (Rees *et al.* 1995), $I_{K,ATP}$ (Priebe & Beuckelmann, 1998) and $I_{Cl,ir}$ (Duan *et al.* 2000), have been previously reported to be responsible for the hyposmotic cell swelling-induced changes in membrane ion permeability and various cellular functions, including cardiac electrical activity and contractility (Vandenberg *et al.* 1996; Wright & Rees, 1998; Befroy *et al.* 1999; Kocic *et al.* 2001; Baumgarten & Clemo, 2003; Frey *et al.* 2004). It has been recently reported that volume-regulated K^+ transport or flux across the plasma membrane plays a crucial role in the regulation of the apoptotic volume decrease and programmed cell death (apoptosis) (Remillard & Yuan, 2004). Increasing evidence suggests that apoptosis may be

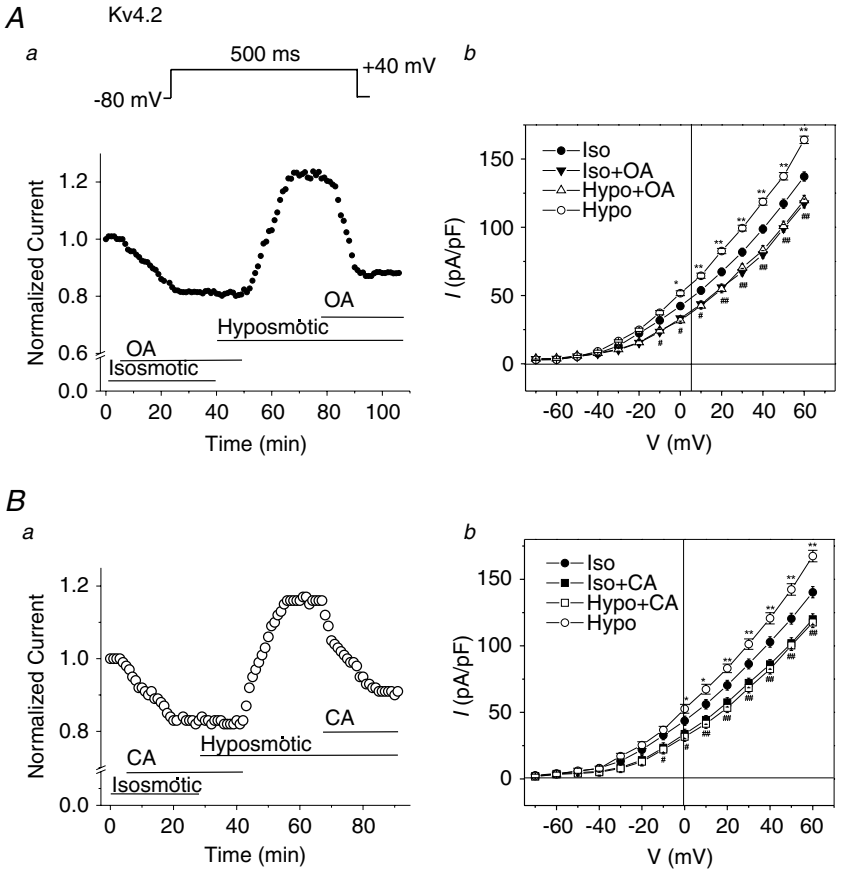

Figure 10. Effects of serine/threonine phosphatase inhibitors on volume regulation of K_v4.2 currents in NIH/3T3 cells

A, effect of OA (100 nM) on peak K_v4.2 currents. *a*, time course of changes in normalized peak K_v4.2 currents measured at +40 mV under isosmotic, isosmotic + OA, and hyposmotic + OA conditions. *b*, *I–V* curves of K_v4.2 channels ($n = 5$) recorded using a protocol as described in Fig. 5 in isosmotic (Iso), isosmotic + OA (Iso + PDBu), and hyposmotic + OA (Hypo + OA) solutions. OA inhibited the currents under isosmotic conditions and prevented further activation by hyposmotic cell swelling. *B*, effects of CA (20 nM) on K_v4.2 channels.

a, time course of changes in normalized peak K_v4.2 currents recorded at +40 mV under isosmotic, isosmotic + CA, and hyposmotic + CA conditions. *b*, mean *I–V* curves of K_v4.2 channels ($n = 5$) in isosmotic (Iso), isosmotic + CA (Iso + CA), and hyposmotic + CA (Hypo + BIM) solutions. CA inhibited the currents under isosmotic conditions and prevented further activation by hyposmotic cell swelling.

a driving force in the transition from compensated hypertrophy to failure in the work-overloaded myocardium. In this study we found that $I_{to,fast}$ is regulated by cell volume changes and cell swelling-induced up-regulation of $I_{to,fast}$ may be responsible for the shortening in early (phase 1) repolarization of cardiac APD of mouse ventricular myocytes. These findings strongly suggest a novel role of $K_v4.2/4.3$ channels in cell volume regulation and may also provide an alternative mechanism for the link between electrical remodelling and structural remodelling of the heart under pathological conditions such as myocardial hypertrophy, heart failure, hypoxia, ischaemia and reperfusion.

Molecular mechanisms responsible for volume regulation of $I_{to,fast}$ in mouse heart

The molecular basis of voltage-dependent outward K^+ currents in native cardiac myocytes is very complicated and may vary in different species and in different regions and cell types of the same heart (Wang *et al.* 1999; Nerbonne & Guo, 2002; Zicha *et al.* 2003; Decher *et al.* 2004). At least five outward K^+ currents ($I_{to,fast}$, $I_{to,slow}$, $I_{K,slow1}$, $I_{K,slow2}$ and I_{ss}) concomitantly exist in native adult mouse heart, and it is difficult to efficiently separate and accurately assess each component (Xu *et al.* 1999*b*; Guo *et al.* 2000; London *et al.* 2001; Zhou *et al.* 2003). $I_{to,fast}$ is present in all left ventricular apex cells and in most left ventricular septum cells, whereas $I_{to,slow}$ is identified only in left ventricular septum cells (Xu *et al.* 1999*b*; Guo *et al.* 2000). $I_{K,slow}$, and I_{ss} exhibit their molecular properties different from either $I_{to,fast}$ or $I_{to,slow}$. It is believed that $I_{to,slow}$ may be encoded by $K_v1.4$ α-subunit (Guo *et al.* 2000), while $I_{K,slow}$ may be encoded by $K_v1.5$ ($I_{K,slow1}$) and $K_v2.1$ ($I_{K,slow2}$) (Xu *et al.* 1999*b*; Zhou *et al.* 2003). In the present study we used a combination of voltage protocol and pharmacological tools as previously described to selectively separate $I_{to,fast}$ from other K^+ currents in mouse cardiac myocytes (Brouillette *et al.* 2004). We found that $I_{to,fast}$, but not I_{ss} was regulated by changes in cell volume.

Both $K_v4.2$ and $K_v4.3$ have been suggested to be major molecular subunits in the formation of $I_{to,fast}$ in cardiac myocytes of many species (Kaab *et al.* 1998; Wang *et al.* 1999; Nerbonne & Guo, 2002). Functional channels underlying mouse ventricular $I_{to,fast}$ may be a heteromultimer of $K_v4.2/4.3$ α-subunits assembling with auxiliary subunits (e.g. K_v channel-interacting protein 2 (KChIP2)) (Guo *et al.* 2002), it is still, however, difficult to reproduce the exact functional channel for endogenous $I_{to,fast}$ in the heterologous expression system by simply expressing these genes together since no information is currently available regarding the exact composition of these subunits for the functional channels in terms of the numbers for each subunits and the isoforms of KChIP2. On the other hand, in most species studied to date, I_{to} is encoded by either $K_v4.2$ or $K_v4.3$, not always by a combination of the two. The recent identification by Sanguinetti's laboratory of new isoforms of KChIP2 in the heart clearly showed that the functional diversity of the I_{to} is far more complicated than people have thought (Decher *et al.* 2004). Obviously, it would be extremely difficult to study a particular KChIP2 isoform and its combination with $K_v4.2$ or $K_v4.3$ or both. Nevertheless, our results on both $K_v4.2$ and $K_v4.3$ channels suggest that the regulation of the channels by cell volume may be essentially through modulation of the α-subunits because the properties of the regulation of these expressed $K_v4.2/4.3$ channels in NIH/3T3 cells are almost identical to those of their native functional correlate $I_{to,fast}$, in terms of voltage-dependent activation and inactivation, recovery from inactivation, and sensitivity to osmotic stress, PKC and phosphatase. Our results also further support the notion that $K_v4.2$ and $K_v4.3$ are major components responsible for $I_{to,fast}$ in native mouse ventricular myocytes.

Numerous previous studies have clearly demonstrated that cell swelling induces protein dephosphorylation whereas cell shrinkage causes protein phosphorylation in a variety of cell systems, including epithelial (Haas *et al.* 1995) and endothelial (Klein *et al.* 1993) cells, erythrocytes (Lytle, 1998), Ehrlich mouse ascites tumour cells (Larsen *et al.* 1994), cardiac myocytes (Duan *et al.* 1995, 1999*a*; Hall *et al.* 1995) and vascular smooth muscle cells (Zhong *et al.* 2002). For example, phosphorylation/dephosphorylation processes mediated by PKC and phosphatases may be critically involved in the osmotic regulation of volume-regulated Cl^- currents encoded by genes of the CIC chloride channel family (ClC-3) ($I_{Cl,vol}$) (Duan *et al.* 1995, 1999*a*; Zhong *et al.* 2002; Baumgarten & Clemo, 2003) or ClC-2 ($I_{Cl,ir}$) (Rutledge *et al.* 2001). In this study we found that the osmotic regulation of endogenous $I_{to,fast}$ and its molecular correlates $K_v4.2$ and $K_v4.3$ channels is also coupled to activities of PKC and phosphatases. To date, at least seven isoforms have been identified in mammalian cardiac myocytes, including α, β, δ, ε, η, ι and ζ. Among Ca^{2+}-independent, novel PKCs, δ, ε, and η are expressed in the heart (Schreiber *et al.* 2001). Both Ca^{2+}-sensitive (PKCα) and -insensitive (PKCδ and PKCε) PKC isozymes are abundantly expressed in NIH/3T3 cells (Szallasi *et al.* 1994). Similar to our previous observations, the effect of cell swelling on $I_{to,fast}$ was also studied under experimental conditions where $[Ca^{2+}]_i$ is strongly buffered by EGTA (10 mM) to separate the Ca^{2+}-independent $I_{to,fast}$ from other Ca^{2+}-dependent currents such as $I_{Cl,Ca}$. Therefore, our results indicate a prominent role for Ca^{2+}-independent signalling pathways, such as Ca^{2+}-independent PKC isoforms, in the mechanism of cell volume regulation of $I_{to,fast}$ in the mouse heart. It has been found that in both fetal and adult mouse ventricles the majority of PKC activity was Ca^{2+} independent (Schreiber *et al.*

2001). Immunoprecipitation assays indicated that PKCδ and PKCε were responsible for the majority of the Ca^{2+}-independent activity in mouse ventricles (Schreiber *et al.* 2001). Therefore, both isoforms may be involved in the regulation of $I_{to,fast}$ in mouse heart. Previous studies by Zhong *et al.* clearly demonstrated that hypotonic cell swelling is accompanied by translocation of PKCϵ from the vicinity of the membrane to cytoplasmic and perinuclear locations, which may be responsible for the cell volume regulation of the volume-regulated Cl^- channels in the vascular smooth muscle cells (Zhong *et al.* 2002). PKCϵ has been found to directly modulate I_{to}. The transmural differences in the subcellular expression of PKCϵ also parallel the transmural gradient of I_{to} (Thorneloe *et al.* 2001*b*). The basal level of ion channel activity under isosmotic conditions may be determined by the balance between basal activities of protein kinases (e.g. PKC) and phosphatases (e.g. PP1/2A), as is the case in $I_{Cl,vol}$ or ClC-3 channels (Duan *et al.* 1995, 1999*a*; Zhong *et al.* 2002; Baumgarten & Clemo, 2003). These results provide further evidence that protein kinase(s)/phosphatase(s)-mediated protein phosphorylation and dephosphorylation may be a common signal transduction pathway for the cellular response to cell volume changes that directly control the function of proteins such as ion channels.

It is very important to know how changes in cell volume regulate channel activity in terms of voltage-dependent gating properties and/or conformational changes of the channel proteins after phosphorylation or dephosphorylation. Po *et al.* (2001) reported that PKC phosphorylation shifts steady-state inactivation of human K_v4.3L while others have reported that PKC inhibits rat K_v4.2 and K_v4.3 and native I_{to} in rat cardiac myocytes without change in their steady-state inactivation properties (Nakamura *et al.* 1997; Shimoni & Liu, 2003). We hypothesized that hyposmotic challenge may activate $I_{to,fast}$ (or K_v4.2/4.3 channels) by affecting its voltage-dependent gating properties through dephosphorylation of the channel protein due to: inactivation of one or more PKC isoforms or other protein kinases; or activation of phosphotases. In this study therefore we carefully studied the effects of osmotic shock on the voltage-dependent gating properties of both endogenous $I_{to,fast}$ in native ventricular myocytes and K_v4.2 and K_v4.3 channels expressed in NIH/3T3 cells. The results indicate that the activation of the K_v4.2/4.3 channels and endogenous $I_{to,fast}$ by hyposmotic cell swelling was voltage independent and no changes in the activation, inactivation and recovery from inactivation were observed. Our results are consistent with those of Nakamura *et al.* (1997) and Shimoni and Liu (2003) but different from those of Po *et al.* (2001). The possible explanations for the discrepancy between these studies may be due to different variants of Kv4.3 (e.g. K_v4.3L *versus* K_v4.3S) between human and rat and/or different expression systems. At this point, it is still not known how osmotic challenge-induced phosphorylation or dephosphorylation of the K_v4.2/4.3 channels causes closing or opening of the channels, respectively. Direct measurement of changes in the activity of kinases and/or phosphatases and biochemical evidence for phosphorylation of K_v4.2 or K_v4.3 channels during alterations of cell volume are needed to further validate whether hyposmotic challenge and PDBu treatment act on the same site. In the case of ClC-3 channels, it seems that phosphorylation/dephosphorylation of the N-terminus is the key link between cell swelling and channel opening (Duan *et al.* 1999*a*). It is therefore reasonable to propose mutation experiments on the consensus PKC phosphorylation sites to test directly whether phosphorylation and dephosphorylation are linked to cell volume regulation, as in the case of ClC-3 channels (Duan *et al.* 1999*a*). There are, however, numerous consent PKC phosphorylation sites in rat long form K_v4.3 (Kv4.3L) and K_v4.2, respectively. It would be an extremely difficult task to identify which amino acid would need to be mutated to yield meaningful phenotypes. It should also be pointed out that it is possible that phosphorylation and dephosphorylation of the channel protein may cause conformational changes to prevent further regulation by changes in cell volume, which may not necessarily be linked to the signal transduction pathways of osmotic stress. Therefore, the mutation experiments were not performed in this study.

In the intact heart the mechanism of channel activation by cell swelling may be more complicated than in the isolated individual cells described here. For instance, there are many aspects of heterogeneity across the left ventricular wall. In addition to the regional differences in the expression of K_v currents or the K_v subunits (K_v4.2, K_v4.3, KChIP2, K_v1.5, K_v2.1) encoding these currents in adult male and female mouse ventricles (Brunet *et al.* 2004), the transmural gradient in PKC isozymes (e.g. PKCε) across the ventricular wall has been described in rat heart (Thorneloe *et al.* 2001*a*; Shimoni & Liu, 2003).The electrophysiological heterogeneity in the transmural myocardium of the murine left ventricle may become even more complex due to significant remodelling under pathological conditions (Thorneloe *et al.* 2001*a*; Shimoni & Liu, 2003; Zicha *et al.* 2003). It is thus very possible that under some pathological conditions like hypertrophy and ischaemia, the regulation of $I_{to,fast}$ may be significantly remodelled along with differential subcellular expression and activation of PKC isozymes in the heart. In fact, the transmural heterogeneity in I_{to} has been suggested to contribute to arrhythmogenesis and change in contractile states during the pathological progression of hypertrophy and heart failure (Oudit *et al.*

2001; Li *et al.* 2002), myocardial ischaemia and infarction (Kaprielian *et al.* 2002) and Brugada syndrome (Di Diego *et al.* 2002). Therefore, whether the mechanisms for the regulation of $K_v4.2/4.3$ channels described in this study are applicable in the intact heart and what the consequences of the volume regulation of these channels are under physiological or pathological situations need to be further investigated at an integrated level.

Significance

Although changes in $K_v4.2/4.3$ channels have been correlated to electrical remodelling in many heart diseases including myocardial ischaemia and infarction (Huang *et al.* 2000) and cardiac hypertrophy and failure (Sah *et al.* 2003), possible involvement of $K_v4.2/4.3$ channels in the initiation and development of heart disease remains to be elucidated. Our results provide the first evidence that cardiac $K_v4.2/4.3$ channels can be regulated by cell volume and strongly suggest that $I_{to,fast}$ may be an important pathological substrate associated with osmotic challenges and cell volume changes. These findings are important because the osmotic-stress regulation of $I_{to,fast}$ may represent a novel mechanism for many important cellular functions, including cell proliferation and apoptosis (Wright & Rees, 1998; Lang *et al.* 2000; Kocic *et al.* 2001; Baumgarten & Clemo, 2003; Remillard & Yuan, 2004) which are involved not only in cardiac cells but also in many other cell types in the context of health and disease. Therefore, these data may provide new insight into our understanding of the role of $K_v4.2/4.3$ in adaptive remodelling in response to physiological and pathophysiological stresses associated with osmotic challenges and cell volume perturbations.

References

Barry DM, Xu H, Schuessler RB & Nerbonne JM (1998). Functional knockout of the transient outward current, long-QT syndrome, and cardiac remodeling in mice expressing a dominant-negative Kv4 alpha subunit. *Circ Res* **83**, 560–567.

Baumgarten CM & Clemo HF (2003). Swelling-activated chloride channels in cardiac physiology and pathophysiology. *Prog Biophys Mol Biol* **82**, 25–42.

Befroy DE, Powell T, Radda GK & Clarke K (1999). Osmotic shock: modulation of contractile function, pHi, and ischemic damage in perfused guinea pig heart. *Am J Physiol* **276**, H1236–H1244.

Brouillette J, Clark RB, Giles WR & Fiset C (2004). Functional properties of K^+ currents in adult mouse ventricular myocytes. *J Physiol* **559**, 777–798.

Brunet S, Aimond F, Li H, Guo W, Eldstrom J, Fedida D, Yamada KA & Nerbonne JM (2004). Heterogeneous expression of repolarizing, voltage-gated K^+ currents in adult mouse ventricles. *J Physiol* **559**, 103–120.

Caballero R, Gomez R, Moreno I, Nunez L, Gonzalez T, Arias C, Guizy M, Valenzuela C, Tamargo J & Delpon E (2004). Interaction of angiotensin II with the angiotensin type 2 receptor inhibits the cardiac transient outward potassium current. *Cardiovasc Res* **62**, 86–95.

Cohen P (1992). Signal integration at the level of protein kinases, protein phosphatases and their substrates. *Trends Biochem Sci* **17**, 408–413.

Decher N, Barth AS, Gonzalez T, Steinmeyer K & Sanguinetti MC (2004). Novel KChIP2 isoforms increase functional diversity of transient outward potassium currents. *J Physiol* **557**, 761–772.

Di Diego JM, Cordeiro JM, Goodrow RJ, Fish JM, Zygmunt AC, Perez GJ, Scornik FS & Antzelevitch C (2002). Ionic and cellular basis for the predominance of the Brugada syndrome phenotype in males. *Circulation* **106**, 2004–2011.

Dixon JE, Shi W, Wang HS & McDonald C, Yu H, Wymore RS, Cohen IS & McKinnon D (1996). Role of the Kv4.3 K^+ channel in ventricular muscle. A molecular correlate for the transient outward current. *Circ Res* **79**, 659–668.

Dorn GW & Force T (2005). Protein kinase cascades in the regulation of cardiac hypertrophy. *J Clin Invest* **115**, 527–537.

Duan D, Cowley S, Horowitz B & Hume JR (1999*a*). A serine residue in Clc-3 links phosphorylation-dephosphorylation to chloride channel regulation by cell. *J Gen Physiol* **113**, 57–70.

Duan D, Fermini B & Nattel S (1993). Potassium channel blocking properties of propafenone in rabbit atrial myocytes. *J Pharmacol Exp Ther* **264**, 1113–1123.

Duan D, Fermini B & Nattel S (1995). Alpha-adrenergic control of volume-regulated Cl^- currents in rabbit atrial myocytes. Characterization of a novel ionic regulatory mechanism. *Circ Res* **77**, 379–393.

Duan D & Hume JR (2000). NO and the regulation of VSOACs. *J Physiol* **528**, 2.

Duan D, Hume JR & Nattel S (1997*a*). Evidence that outwardly rectifying Cl^- channels underlie volume-regulated Cl^- currents in heart. *Circ Res* **80**, 103–113.

Duan D, Liu LL, Bozeat N, Huang ZM, Xiang SY, Wang GL, Ye L & Hume JR (2005). Functional role of anion channels in cardiac diseases. *Acta Pharmacol Sin* **26**, 265–278.

Duan D, Winter C, Cowley S, Hume JR & Horowitz B (1997*b*). Molecular identification of a volume-regulated chloride channel. *Nature* **390**, 417–421.

Duan D, Ye L, Britton F, Horowitz B & Hume JR (2000). A novel anionic inward rectifier in native cardiac myocytes. *Circ Res* **86**, E63–E71.

Duan D, Ye L, Britton F, Miller LJ, Yamazaki J, Horowitz B & Hume JR (1999*b*). Purinoceptor-coupled Cl^- channels in mouse heart: a novel, alternative pathway for CFTR regulation. *J Physiol* **521**, 43–56.

Ellershaw DC, Greenwood IA & Large WA (2000). Dual modulation of swelling-activated chloride current by NO and NO donors in rabbit portal vein myocytes. *J Physiol* **528**, 15–24.

Ellershaw DC, Greenwood IA & Large WA (2002). Modulation of volume-sensitive chloride current by noradrenaline in rabbit portal vein myocytes. *J Physiol* **542**, 537–547.

Frey N, Katus HA, Olson EN & Hill JA (2004). Hypertrophy of the heart: a new therapeutic target? *Circulation* **109**, 1580–1589.

Guo W, Li H, Aimond F, Johns DC, Rhodes KJ, Trimmer JS & Nerbonne JM (2002). Role of heteromultimers in the generation of myocardial transient outward K^+ currents. *Circ Res* **90**, 586–593.

Guo W, Li H, London B & Nerbonne JM (2000). Functional consequences of elimination of i(to,f) and i(to,s): early afterdepolarizations, atrioventricular block, and ventricular arrhythmias in mice lacking Kv1.4 and expressing a dominant-negative Kv4 alpha subunit. *Circ Res* **87**, 73–79.

Haas M, McBrayer D & Lytle C (1995). $[Cl^-]_i$-dependent phosphorylation of the Na-K-Cl cotransport protein of dog tracheal epithelial cells. *J Biol Chem* **270**, 28955–28961.

Hall SK, Zhang J & Lieberman M (1995). Cyclic AMP prevents activation of a swelling-induced chloride-sensitive conductance in chick heart cells. *J Physiol* **488**, 359–369.

Hamill OP, Huguenard JR & Prince DA (1991). Patch-clamp studies of voltage-gated currents in identified neurons of the rat cerebral cortex. *Cereb Cortex* **1**, 48–61.

Hatano N, Ohya S, Muraki K, Giles W & Imaizumi Y (2003). Dihydropyridine Ca^{2+} channel antagonists and agonists block Kv4.2, Kv4.3 and Kv1.4 K^+ channels expressed in HEK293 cells. *Br J Pharmacol* **139**, 533–544.

Herzig S & Neumann J (2000). Effects of serine/threonine protein phosphatases on ion channels in excitable membranes. *Physiol Rev* **80**, 173–210.

Hiraoka M, Kawano S, Hirano Y & Furukawa T (1998). Role of cardiac chloride currents in changes in action potential characteristics and arrhythmias. *Cardiovasc Res* **40**, 23–33.

Hoppe UC, Marban E & Johns DC (2000). Molecular dissection of cardiac repolarization by in vivo Kv4.3 gene transfer. *J Clin Invest* **105**, 1077–1084.

Huang B, Qin D & El Sherif N (2000). Early down-regulation of K^+ channel genes and currents in the postinfarction heart. *J Cardiovasc Electrophysiol* **11**, 1252–1261.

Hume JR, Duan D, Collier ML, Yamazaki J & Horowitz B (2000). Anion transport in heart. *Physiol Rev* **80**, 31–81.

Hunter T (1995). Protein kinases and phosphatases: the yin and yang of protein phosphorylation and signaling. *Cell* **80**, 225–236.

Ishihara H, Martin BL, Brautigan DL, Karaki H, Ozaki H, Kato Y, Fusetani N, Watabe S, Hashimoto K & Uemura D (1989). Calyculin A and okadaic acid: inhibitors of protein phosphatase activity. *Biochem Biophys Res Commun* **159**, 871–877.

Jennings ML & Schulz RK (1991). Okadaic acid inhibition of KCl cotransport. Evidence that protein dephosphorylation is necessary for activation of transport by either cell swelling or N-ethylmaleimide. *J Gen Physiol* **97**, 799–817.

Johns DC, Nuss HB & Marban E (1997). Suppression of neuronal and cardiac transient outward currents by viral gene transfer of dominant-negative Kv4.2 constructs. *J Biol Chem* **272**, 31598–31603.

Kaab S, Dixon J, Duc J, Ashen D, Nabauer M, Beuckelmann DJ, Steinbeck G, McKinnon D & Tomaselli GF (1998). Molecular basis of transient outward potassium current downregulation in human heart failure: a decrease in Kv4.3 mRNA correlates with a reduction in current density. *Circulation* **98**, 1383–1393.

Kaprielian R, Sah R, Nguyen T, Wickenden AD & Backx PH (2002). Myocardial infarction in rat eliminates regional heterogeneity of AP profiles, I_{to} K^+ currents, and $[Ca^{2+}]_i$ transients. *Am J Physiol Heart Circ Physiol* **283**, H1157–H1168.

Kassiri Z, Zobel C, Nguyen TT, Molkentin JD & Backx PH (2002). Reduction of I_{to} causes hypertrophy in neonatal rat ventricular myocytes. *Circ Res* **90**, 578–585.

Klein JD, Perry PB & O'Neill WC (1993). Regulation by cell vlume of Na^+–K^+–$2Cl^-$ cotransport in vascular endothelial cells: role of protein phosphorylation. *J Membr Biol* **132**, 243–252.

Kocic I, Hirano Y & Hiraoka M (2001). Ionic basis for membrane potential changes induced by hypoosmotic stress in guinea-pig ventricular myocytes. *Cardiovasc Res* **51**, 59–70.

Lang F, Busch GL, Ritter M, Volkl H, Waldegger S, Gulbins E & Haussinger D (1998). Functional significance of cell volume regulatory mechanisms. *Physiol Rev* **78**, 247–306.

Lang F, Ritter M, Gamper N, Huber S, Fillon S, Tanneur V, Lepple-Wienhues A, Szabo I & Gulbins E (2000). Cell volume in the regulation of cell proliferation and apoptotic cell death. *Cell Physiol Biochem* **10**, 417–428.

Larsen AK, Jensen BS & Hoffmann EK (1994). Activation of protein kinase C during cell volume regulation in Ehrlich mouse ascites tumor cells. *Biochim Biophys Acta* **1222**, 477–482.

Li GR, Lau CP, Ducharme A, Tardif JC & Nattel S (2002). Transmural action potential and ionic current remodeling in ventricles of failing canine hearts. *Am J Physiol Heart Circ Physiol* **283**, H1031–H1041.

London B, Guo W, Pan X, Lee JS, Shusterman V, Rocco CJ, Logothetis DA, Nerbonne JM & Hill JA (2001). Targeted replacement of Kv1.5 in the mouse leads to loss of the 4-aminopyridine-sensitive component of $I_{K,slow}$ and resistance to drug-induced qt prolongation. *Circ Res* **88**, 940–946.

Lytle C (1998). A volume-sensitive protein kinase regulates the Na-K-2Cl cotransporter in duck red blood cells. *Am J Physiol* **274**, C1002–C1010.

Nakamura TY, Coetzee WA, Vega-Saenz d. M, Artman M & Rudy B (1997). Modulation of Kv4 channels, key components of rat ventricular transient outward K^+ current, by PKC. *Am J Physiol* **273**, H1775–H1786.

Nerbonne JM & Guo W (2002). Heterogeneous expression of voltage-gated potassium channels in the heart: roles in normal excitation and arrhythmias. *J Cardiovasc Electrophysiol* **13**, 406–409.

Ohya S, Tanaka M, Oku T, Asai Y, Watanabe M, Giles WR & Imaizumi Y (1997). Molecular cloning and tissue distribution of an alternatively spliced variant of an A-type K^+ channel alpha-subunit, Kv4.3 in the rat. *FEBS Lett* **420**, 47–53.

Oudit GY, Kassiri Z, Sah R, Ramirez RJ, Zobel C & Backx PH (2001). The molecular physiology of the cardiac transient outward potassium current (I_{to}) in normal and diseased myocardium. *J Mol Cell Cardiol* **33**, 851–872.

Po SS, Wu RC, Juang GJ, Kong W & Tomaselli GF (2001). Mechanism of alpha-adrenergic regulation of expressed hKv4.3 currents. *Am J Physiol Heart Circ Physiol* **281**, H2518–H2527.

Priebe L & Beuckelmann DJ (1998). Cell swelling causes the action potential duration to shorten in guinea-pig ventricular myocytes by activating $I_{K,ATP}$. *Pflugers Arch* **436**, 894–898.

Rees SA, Vandenberg JI, Wright AR, Yoshida A & Powell T (1995). Cell swelling has differential effects on the rapid and slow components of delayed rectifier potassium current in guinea pig cardiac myocytes. *J Gen Physiol* **106**, 1151–1170.

Remillard CV & Yuan JX (2004). Activation of K^+ channels: an essential pathway in programmed cell death. *Am J Physiol Lung Cell Mol Physiol* **286**, L49–L67.

Rutledge E, Bianchi L, Christensen M, Boehmer C, Morrison R, Broslat A, Beld AM, George AL, Greenstein D & Strange K (2001). CLH-3, a ClC-2 anion channel ortholog activated during meiotic maturation in C. *elegans* oocytes. *Curr Biol* **11**, 161–170.

Sah R, Ramirez RJ, Oudit GY, Gidrewicz D, Trivieri MG, Zobel C & Backx PH (2003). Regulation of cardiac excitation–contraction coupling by action potential repolarization: role of the transient outward potassium current (I_{to}). *J Physiol* **546**, 5–18.

Schreiber KL, Paquet L, Allen BG & Rindt H (2001). Protein kinase C isoform expression and activity in the mouse heart. *Am J Physiol Heart Circ Physiol* **281**, H2062–H2071.

Shimoni Y & Liu XF (2003). Role of PKC in autocrine regulation of rat ventricular K^+ currents by angiotensin and endothelin. *Am J Physiol Heart Circ Physiol* **284**, H1168–H1181.

Steenbergen C, Hill ML & Jennings RB (1985). Volume regulation and plasma membrane injury in aerobic, anaerobic, and ischemic myocardium in vitro. Effects of osmotic cell swelling on plasma membrane integrity. *Circ Res* **57**, 864–875.

Szallasi Z, Smith CB, Pettit GR & Blumberg PM (1994). Differential regulation of protein kinase C isozymes by bryostatin 1 and phorbol 12-myristate 13-acetate in NIH 3T3 fibroblasts. *J Biol Chem* **269**, 2118–2124.

Takimoto K, Li D, Hershman KM, Li P, Jackson EK & Levitan ES (1997). Decreased expression of Kv4.2 and novel Kv4.3 K^+ channel subunit mRNAs in ventricles of renovascular hypertensive rats. *Circ Res* **81**, 533–539.

Thorneloe KS, Liu XF, Walsh MP & Shimoni Y (2001*a*). Transmural differences in rat ventricular protein kinase C epsilon correlate with its functional regulation of a transient cardiac K^+ current. *J Physiol* **533**, 145–154.

Thorneloe KS, Liu XF, Walsh MP & Shimoni Y (2001*b*). Transmural differences in rat ventricular protein kinase C epsilon correlate with its functional regulation of a transient cardiac K^+ current. *J Physiol* **533**, 145–154.

Vandenberg JI, Bett GC & Powell T (1997). Contribution of a swelling-activated chloride current to changes in the cardiac action potential. *Am J Physiol* **273**, C541–C547.

Vandenberg JI, Rees SA, Wright AR & Powell T (1996). Cell swelling and ion transport pathways in cardiac myocytes. *Cardiovasc Res* **32**, 85–97.

Wang Z, Feng J, Shi H, Pond A, Nerbonne JM & Nattel S (1999). Potential molecular basis of different physiological properties of the transient outward K^+ current in rabbit and human atrial myocytes. *Circ Res* **84**, 551–561.

Wright AR & Rees SA (1998). Cardiac cell volume: crystal clear or murky waters? A comparison with other cell types. *Pharmacol Ther* **80**, 89–121.

Xu H, Barry DM, Li H, Brunet S, Guo W & Nerbonne JM (1999*a*). Attenuation of the slow component of delayed rectification, action potential prolongation, and triggered activity in mice expressing a dominant-negative Kv2 alpha subunit. *Circ Res* **85**, 623–633.

Xu H, Guo W & Nerbonne JM (1999*b*). Four kinetically distinct depolarization-activated K^+ currents in adult mouse ventricular myocytes. *J Gen Physiol* **113**, 661–678.

Xu H, Li H & Nerbonne JM (1999*c*). Elimination of the transient outward current and action potential prolongation in mouse atrial myocytes expressing a dominant negative Kv4 alpha subunit. *J Physiol* **519**, 11–21.

Xu Y, Dong PH, Zhang Z, Ahmmed GU & Chiamvimonvat N (2002). Presence of a calcium-activated chloride current in mouse ventricular myocytes. *Am J Physiol Heart Circ Physiol* **283**, H302–H314.

Yue L, Melnyk P, Gaspo R, Wang Z & Nattel S (1999). Molecular mechanisms underlying ionic remodeling in a dog model of atrial fibrillation. *Circ Res* **84**, 776–784.

Zhong J, Wang GX, Hatton WJ, Yamboliev IA, Walsh MP & Hume JR (2002). Regulation of volume-sensitive outwardly rectifying anion channels in pulmonary arterial smooth muscle cells by PKC. *Am J Physiol Cell Physiol* **283**, C1627–C1636.

Zhou J, Kodirov S, Murata M, Buckett PD, Nerbonne JM & Koren G (2003). Regional upregulation of Kv2.1-encoded current, $I_{K,slow2}$, in Kv1DN mice is abolished by crossbreeding with Kv2DN mice. *Am J Physiol Heart Circ Physiol* **284**, H491–H500.

Zicha S, Moss I, Allen B, Varro A, Papp J, Dumaine R, Antzelevich C & Nattel S (2003). Molecular basis of species-specific expression of repolarizing K^+ currents in the heart. *Am J Physiol Heart Circ Physiol* **285**, H1641–H1649.

Acknowledgements

We are very grateful to Drs Susumu Ohya and Yuji Imaizumi (Department of Molecular & Cellular Pharmacology, Nagoya City University, Japan) for the generous gift of Kv4.2 and Kv4.3 cDNA. This study was supported by NIH (HL63914) and NCRR (P20 RR15581). G.-L.W. is a postdoctoral fellow of the American Heart Association, Western States Affiliate.

Author's present address

G.-L. Wang: Department of Pharmacology, Zhongshan Medical College, Sun Yat-Sen University, 74 Zhongshan 2nd Road, Guangzhou, People's Republic of China 510080.